Elsevier Editorial System(tm) for Journal of Colloid and Interface Science

Manuscript Draft

Manuscript Number: JCIS-16-1863R1

Title: Nanocrystallinity effects on osteoblast and osteoclast response to silicon substituted hydroxyapatite

Article Type: Full length article

Section/Category: E. Biomaterials and Nanomedicine

Keywords: nanocrystallinity; hydroxyapatite; silicon; osteoclast; osteoblast; anoikis; osteoporosis; cell adhesión; apoptosis; cell cycle.

Corresponding Author: Prof. Maria Teresa Portolés, Professor, PhD

Corresponding Author's Institution: Faculty of Chemistry, Universidad Complutense

First Author: Laura Casarrubios

Order of Authors: Laura Casarrubios; María Concepción Matesanz, PhD; Sandra Sánchez-Salcedo, PhD; Daniel Arcos, PhD; María Vallet-Regí, Professor, PhD; Maria Teresa Portolés, Professor, PhD

Abstract: Hypothesis: Silicon substituted hydroxyapatites (SiHA) are highly crystalline bioceramics treated at high temperatures (about 1200°C) which have been approved for clinical use with spinal, orthopedic, periodontal, oral and craniomaxillofacial applications. The preparation of SiHA with lower temperature methods (about 700°C) provides nanocrystalline SiHA (nano-SiHA) with enhanced bioreactivity due to higher surface area and smaller crystal size. The aim of this study has been to know the nanocrystallinity effects on the response of both osteoblasts and osteoclasts (the two main cell types involved in bone remodelling) to silicon substituted hydroxyapatite.
Experiments: Saos-2 osteoblasts and osteoclast-like cells (differentiated from RAW-264.7 macrophages) have been cultured on the surface of nano-SiHA and SiHA disks and different cell parameters have been evaluated: cell adhesion, proliferation, viability, intracellular content of reactive oxygen species, cell cycle phases, apoptosis, cell morphology, osteoclast-like cell differentiation and resorptive activity.
Findings: This comparative in vitro study evidences that nanocrystallinity of SiHA affects the cell/biomaterial interface inducing bone cell apoptosis by loss of cell anchorage (anoikis), delaying osteoclast-like cell differentiation and decreasing the resorptive activity of this cell type. These results suggest the potential use of nano-SiHA biomaterial for preventing bone resorption in treatment of osteoporotic bone.

Madrid, 27-July-2016

Dear Editor:

Concerning our previous manuscript JCIS-16-1863 entitled “Nanocrystallinity effects on osteoblast and osteoclast response to silicon substituted hydroxyapatite”, we have taken into account the Editor and Reviewer´s comments to improve the quality of our manuscript, and a detailed list of the changes and the responses to these comments is included below. All these changes have been highlighted in blue in the revised version of the manuscript.

Reviewers' comments:

Editor:

1) Manuscripts published in JCIS must explain the significant advances provided in approaches and understanding compared to previous literature, and/or demonstrate convincingly potential in new applications. The Conclusions of your paper are especially important for this. Therefore, please try to sharpen this further. The optimal Conclusion should include:

* A summary of your key findings.

* A highlight of your hypothesis, new concepts and innovations.

* A summary of key improvements compared to findings in literature [provide a couple of references to indicate key improvements].

* Your vision for future work.

Authors

The authors thank Editor’s comments and criticisms aimed to improve the quality of the manuscript. The authors admit that several important subjects are deficiently explained in the previous version and sincerely believe that the changes introduced in this revised manuscript will satisfy the standards of JCIS. The Conclusion has been rewritten, the positive points of this study have been highlighted, a couple of references have been included to indicate key improvements, and the current and future studies have been indicated in this section.

Reviewer #1: The ms reports in an investigation of nanocrystalinity of silicon-substituted hydroxyapatite on osteoblast and osteoclast response. Although the study provides some nice results, there are some issues which need to be addressed before this ms can be further considered for publication in JCIS:

1) The weakest point of the ms is the unclear conceptual novelty provided. Thus, there have been numerous previous investigations of various HA-based materials, including also effects of crystallinity. The authors therefore need to make a better job in clarifying what conceptual novelty is provided, to motivate the publication of the ms.

Authors

The authors thank Reviewer's criticisms and admit the unclear conceptual novelty provided. The novelty and the great interest of these findings are explained in more detail in the revised version. The Conclusion has been rewritten and the positive points of this study have been highlighted.

2) Surface characterization is insufficient for publication in a surface chemical journal such as JCIS. As a minimum, data on contact angle (advancing and receeding) and surface composition (from XPS or the like) should be included as well.

Authors

The authors agree with the suggestion concerning the chemical analysis and contact angle measurements. In this revised version we have included the EDX spectra to show the chemical composition of the samples surface. We appreciate reviewer´s suggestion and a deeper study by XPS will be carried out in a near future. Regarding contact angle measurements, the results have evidenced clear differences between SiHA and nano-SiHA. Due to the high porosity of nano-SiHA, the drop was absorbed after a few seconds on the surface, so that advancing and receeding tests could not be carried out. Anyway, the data obtained in static conditions put light about the differences between samples. In this sense the authors thank the reviewer for this suggestion.

3) Given the intended use of these materials as biomaterials, further results are needed on cell toxicity and cascade activation (complement, coagulation).

Authors

Concerning the cell toxicity studies, different cell parameters have been evaluated in the present work: cell adhesion, proliferation, viability, intracellular content of reactive oxygen species (ROS), cell cycle phases, apoptosis, cell morphology, osteoclast-like cell differentiation and resorptive activity. All these parameters are enough to evidence the absence of cell toxicity after contact of bone cells with nano-SiHA and SiHA materials.

Concerning cascade activation as coagulation, since fibrinogen is involved in blood clotting, the adsorption of fibrinogen on crystalline and nanocrystalline SiHA was measured in a previous work (Colloids and Surfaces B: Biointerfaces 2015, 133,304–313) showing that the amount of fibrinogen adsorbed on crystalline SiHA was significantly lower than on nanocrystalline SiHA. These previous results concerning adsorption of serum proteins and fibrinogen, which could be related to the implant success and hemocompatibility, and this new reference (39) have been included in the revised version.

4) Although osteoblast and osteoclast responses are related to bone remodeling, the ms contains no direct information on mineralization effects. It would strengthen an already nice paper if some data on this could be included.

Authors

The authors agree with reviewer's suggestion. In vivo mineralization studies with an osteopenic sheep model are currently being carried out for in vivo evaluation of these hydroxyapatites (project from Ministerio de Economía y Competitividad MAT2013-43299-R) and the obtained results will be included in a future manuscript. This fact has been explained in the Conclusion in the revised manuscript.

5) Conclusions are short and non-instructive, and need improvement.

Authors

The Conclusion has been rewritten and the positive points of this study have been highlighted.

I do hope you will consider the revised manuscript suitable for publication in *Journal of Colloid and Interface Science.*

Thanking you very much for your attention, I remain

Sincerely yours

Prof. M. Teresa Portolés
Departamento de Bioquímica y Biología Molecular I
Facultad de Ciencias Químicas
Universidad Complutense, 28040-Madrid, Spain
E-mail: portoles@quim.ucm.es

Madrid, 27-July-2016

Dear Editor:

Concerning our previous manuscript JCIS-16-1863 entitled “Nanocrystallinity effects on osteoblast and osteoclast response to silicon substituted hydroxyapatite”, we have taken into account the Editor and Reviewer´s comments to improve the quality of our manuscript, and a detailed list of the changes and the responses to these comments is included below. All these changes have been highlighted in blue in the revised version of the manuscript.

Reviewers' comments:

Editor:

1) Manuscripts published in JCIS must explain the significant advances provided in approaches and understanding compared to previous literature, and/or demonstrate convincingly potential in new applications. The Conclusions of your paper are especially important for this. Therefore, please try to sharpen this further. The optimal Conclusion should include:

* A summary of your key findings.

* A highlight of your hypothesis, new concepts and innovations.

* A summary of key improvements compared to findings in literature [provide a couple of references to indicate key improvements].

* Your vision for future work.

Authors

The authors thank Editor’s comments and criticisms aimed to improve the quality of the manuscript. The authors admit that several important subjects are deficiently explained in the previous version and sincerely believe that the changes introduced in this revised manuscript will satisfy the standards of JCIS. The Conclusion has been rewritten, the positive points of this study have been highlighted, a couple of references have been included to indicate key improvements, and the current and future studies have been indicated in this section.

Reviewer #1: The ms reports in an investigation of nanocrystalinity of silicon-substituted hydroxyapatite on osteoblast and osteoclast response. Although the study provides some nice results, there are some issues which need to be addressed before this ms can be further considered for publication in JCIS:

1) The weakest point of the ms is the unclear conceptual novelty provided. Thus, there have been numerous previous investigations of various HA-based materials, including also effects of crystallinity. The authors therefore need to make a better job in clarifying what conceptual novelty is provided, to motivate the publication of the ms.

Authors

The authors thank Reviewer's criticisms and admit the unclear conceptual novelty provided. The novelty and the great interest of these findings are explained in more detail in the revised version. The Conclusion has been rewritten and the positive points of this study have been highlighted.

2) Surface characterization is insufficient for publication in a surface chemical journal such as JCIS. As a minimum, data on contact angle (advancing and receeding) and surface composition (from XPS or the like) should be included as well.

Authors

The authors agree with the suggestion concerning the chemical analysis and contact angle measurements. In this revised version we have included the EDX spectra to show the chemical composition of the samples surface. We appreciate reviewer´s suggestion and a deeper study by XPS will be carried out in a near future. Regarding contact angle measurements, the results have evidenced clear differences between SiHA and nano-SiHA. Due to the high porosity of nano-SiHA, the drop was absorbed after a few seconds on the surface, so that advancing and receeding tests could not be carried out. Anyway, the data obtained in static conditions put light about the differences between samples. In this sense the authors thank the reviewer for this suggestion.

3) Given the intended use of these materials as biomaterials, further results are needed on cell toxicity and cascade activation (complement, coagulation).

Authors

Concerning the cell toxicity studies, different cell parameters have been evaluated in the present work: cell adhesion, proliferation, viability, intracellular content of reactive oxygen species (ROS), cell cycle phases, apoptosis, cell morphology, osteoclast-like cell differentiation and resorptive activity. All these parameters are enough to evidence the absence of cell toxicity after contact of bone cells with nano-SiHA and SiHA materials.

Concerning cascade activation as coagulation, since fibrinogen is involved in blood clotting, the adsorption of fibrinogen on crystalline and nanocrystalline SiHA was measured in a previous work (Colloids and Surfaces B: Biointerfaces 2015, 133,304–313) showing that the amount of fibrinogen adsorbed on crystalline SiHA was significantly lower than on nanocrystalline SiHA. These previous results concerning adsorption of serum proteins and fibrinogen, which could be related to the implant success and hemocompatibility, and this new reference (39) have been included in the revised version.

4) Although osteoblast and osteoclast responses are related to bone remodeling, the ms contains no direct information on mineralization effects. It would strengthen an already nice paper if some data on this could be included.

Authors

The authors agree with reviewer's suggestion. In vivo mineralization studies with an osteopenic sheep model are currently being carried out for in vivo evaluation of these hydroxyapatites (project from Ministerio de Economía y Competitividad MAT2013-43299-R) and the obtained results will be included in a future manuscript. This fact has been explained in the Conclusion in the revised manuscript.

5) Conclusions are short and non-instructive, and need improvement.

Authors

The Conclusion has been rewritten and the positive points of this study have been highlighted.

I do hope you will consider the revised manuscript suitable for publication in *Journal of Colloid and Interface Science.*

Thanking you very much for your attention, I remain

Sincerely yours

Prof. M. Teresa Portolés
Departamento de Bioquímica y Biología Molecular I
Facultad de Ciencias Químicas
Universidad Complutense, 28040-Madrid, Spain
E-mail: portoles@quim.ucm.es

*3: Graphical Abstract
Click here to download high resolution image

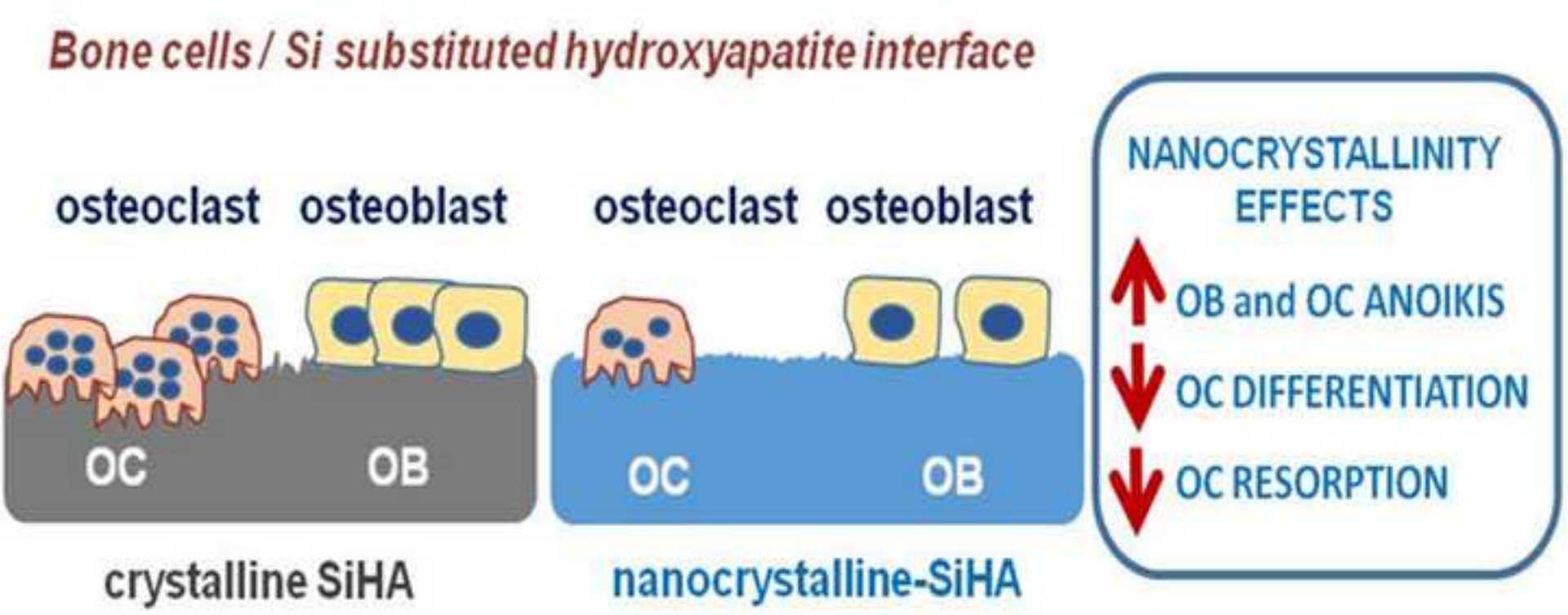

Nanocrystallinity effects on osteoblast and osteoclast response to silicon substituted hydroxyapatite

Laura Casarrubios [a,b], María Concepción Matesanz [a], Sandra Sánchez-Salcedo [c,d], Daniel Arcos [c,d], María Vallet-Regí [c,d], María Teresa Portolés [a,b,*]

[a] Department of Biochemistry and Molecular Biology I/Faculty of Chemistry, Universidad Complutense de Madrid, Spain

[b] Instituto de Investigación Sanitaria San Carlos IdISSC, Spain

portoles@quim.ucm.es, arualanilom@hotmail.com, conchitamatesanz@hotmail.com

[c] Department of Inorganic and Bioinorganic Chemistry/Faculty of Pharmacy, Universidad Complutense de Madrid, Instituto de Investigación Hospital 12 de Octubre i+12, Spain

[d] Networking Research Center on Bioengineering/Biomaterials and Nanomedicine, CIBER-BBN, Spain

vallet@ucm.es, arcosd@ucm.es, sansanch@ucm.es

* Corresponding author: María Teresa Portolés.

E-mail address: portoles@quim.ucm.es

Abstract

Hypothesis: Silicon substituted hydroxyapatites (SiHA) are highly crystalline bioceramics treated at high temperatures (about 1200ºC) which have been approved for clinical use with spinal, orthopedic, periodontal, oral and craniomaxillofacial applications. The preparation of SiHA with lower temperature methods (about 700ºC) provides nanocrystalline SiHA (nano-SiHA) with enhanced bioreactivity due to higher surface area and smaller crystal size. The aim of this study has been to know the nanocrystallinity effects on the response of both osteoblasts and osteoclasts (the two main cell types involved in bone remodelling) to silicon substituted hydroxyapatite.

Experiments: Saos-2 osteoblasts and osteoclast-like cells (differentiated from RAW-264.7 macrophages) have been cultured on the surface of nano-SiHA and SiHA disks and different cell parameters have been evaluated: cell adhesion, proliferation, viability, intracellular content of reactive oxygen species, cell cycle phases, apoptosis, cell morphology, osteoclast-like cell differentiation and resorptive activity.

Findings: This comparative *in vitro* study evidences that nanocrystallinity of SiHA affects the cell/biomaterial interface inducing bone cell apoptosis by loss of cell anchorage (anoikis), delaying osteoclast-like cell differentiation and decreasing the resorptive activity of this cell type. These results suggest the potential use of nano-SiHA biomaterial for preventing bone resorption in treatment of osteoporotic bone.

Keywords: nanocrystallinity, hydroxyapatite, silicon, osteoclast, osteoblast, anoikis, osteoporosis, cell adhesion, apoptosis, cell cycle.

1. Introduction

Bone is a metabolically active and very dynamic tissue in continuous resorption and formation by osteoclasts and osteoblasts respectively, working together via paracrine cell signaling in basic multicellular units (1). Osteoblasts are mononucleated cells which differentiate from mesenchymal stem cells of the bone marrow stroma and are responsible for deposition of bone matrix and regulation of osteoclasts (2,3). Osteoclasts are multinucleated giant cells which differentiate from hematopoietic stem cells (that give rise to monocytes and macrophages) and they perform the bone resorption (4). Osteoclasts attach to the bone surface and initiate resorption by the secretion of hydrogen ions and lysosomal enzymes which degrade all the components of bone matrix producing irregular cavities on the bone surface (5,6). The balance between bone resorption by osteoclasts and bone formation by osteoblasts is influenced by mechanical, genetic, vascular, nutritional, hormonal and local factors. This bone remodeling is necessary to maintain the structural skeleton integrity and mineral homeostasis. Alterations of this process are involved in the pathogenesis of various skeletal diseases, including osteoporosis (7,8).

Silicon (Si) is an essential element for bone and cartilage formation (9-11) and is present in the areas of greatest osteoblastic activity during bone growth (12). This element is essential to the normal development of the glycosaminoglycan network in the extracellular matrix (9), increasing bone collagen content (13). Si also appears to inhibit macrophage and osteoclast activity (14). Bioactive silicate materials upregulate the expression of vascular endothelial growth factor (VEGF) (15), which is involved in both blood vessel and bone formation (16). Small levels of ionic substitution by Si in hydroxyapatite (HA) have been shown to have significant effects on thermal stability, solubility, osteoclastic and osteoblastic response both *in vitro* and *in vivo* (17). Thus, silicon substituted

hydroxyapatite (SiHA) presents enhanced bioactivity *in vivo* than HA, showing beneficial effects in the early stages of bone formation (18). The favourable effects of Si substitution in HA have been explained by considering passive and active mechanisms as material solubility increase, topographical changes, grain size reduction, surface charge modifications and ionic release of Si and Ca, which directly act on bone cells (19-23). All these facts make SiHA very attractive for use as bone substitute material (24-27) and SiHA has recently been incorporated to the biomaterials market as Actifuse ABXTM (Apatech Ltd, UK) for spinal, orthopedic, periodontal, oral and craniomaxillofacial applications. SiHA approved for clinical use are highly crystalline bioceramics treated at high temperatures (about 1200ºC). However, their preparation with lower temperature methods has been suggested to enhance the bioreactivity of these bioceramics (28-30). Avoiding the high temperature sintering process, nanocrystalline pieces and grains can be prepared with higher surface area and smaller crystal size. These characteristics could provide very interesting bioresponses in SiHA since the osteogenic effect of silicon is mainly explained by its location at the crystal boundaries (24,25).

The novelty of the present study is the comparison of the action of nanocrystalline and crystalline silicon substituted hydroxyapatites (nano-SiHA and SiHA respectively) on both osteoblasts and osteoclasts, the two main cell types involved in bone remodelling. In this comparative *in vitro* study, Saos-2 osteoblasts and osteoclast-like cells (differentiated from RAW-264.7 macrophages) have been cultured on the surface of nano-SiHA and SiHA disks and different cell parameters have been evaluated: cell adhesion, proliferation, viability, intracellular content of reactive oxygen species (ROS), cell cycle phases, apoptosis, cell morphology, osteoclast-like cell differentiation and resorptive activity.

2. Materials and methods

2.1 *Synthesis of materials*

Silicon-substituted hydroxyapatite (Si-HA) with nominal formula $Ca_{10}(PO_4)_{5.75}(SiO_4)_{0.25}(OH)_{1.75}\square_{0.25}$, where □ means vacancies at the hydroxyl position, was prepared by aqueous precipitation reaction of $Ca(NO_3)_2{\cdot}4H_2O$, $(NH_4)_2HPO_4$ and $Si(CH_3CH_2O)_4$ solutions. Briefly, a 1 M solution of $Ca(NO_3)_2{\cdot}4H_2O$ was added to a second 0.575 M of $(NH_4)_2HPO_4$ and 0,025 M of $Si(CH_3CH_2O)_4$ solution to obtain the composition described above. The mixture was stirred for 12 h at 80°C. The pH was kept at 9.5 by NH_3 solution addition to ensure constant conditions during the synthesis. The precipitated Si-HA powder was dried, milled and sieved and the powder fraction below 40 μm was selected. Fractions of 300 mg of powder were pressed into disk-shape (11 mm diameter, 2 mm height) by means of 3 tons of uniaxial pressing. Subsequently the discs were treated during 3 hours at 700ºC or 1150ºC resulting in nano-SiHA or SiHA, respectively.

2.2 Characterization of materials

The structural characterization was performed by Powder X-ray diffraction (XRD) in a Philips X'Pert diffractometer equipped with a CuKα radiation (wavelength 1.5406 Å), with a step size of 0.02º 2θ and 8 seconds of counting time. In order to determine the crystalline and microstructural characteristics of both samples, Rietveld refinements were carried out over the XRD patterns collected. The refinements were performed using the atomic position set and the space group of the HA structure P63/m, No. 176 by means of the FullProf 2000 computer program. The instrumental resolution function (IRF) of the diffractometer was obtained from a very-well-crystallized LaB_6 sample and taken into

account in a separate input file. The pseudo-Voigt profile function of Thompson, Cox, and Hastings was used with an asymmetry correction at a low angle.

The contact angles were measured to estimate the wettability of the samples. The experiments were performed by the sessile drop method at 25º C on a CAM 200 KSV contact angle goniometer. Pictures of the drops were taken every 1 s. The software delivered by the instrument manufacturer calculated the contact angles on the basis of a numerical solution of the full Young–Laplace equation.

Textural properties (surface and porosity) were determined by nitrogen adsorption porosimetry in a Micromeritics ASAP 2012. To perform the N_2 adsorption measurements, the samples were previously degassed under vacuum for 24 h at 80ºC. Finally, zeta potential was measured by means of a Zetasizer Nano ZS (Malvern Instruments).

2.3 Culture of osteoblasts in contact with nano-SiHA and SiHA

Human Saos-2 osteoblasts (10^5 cells/ml) were seeded on the surface of nano-SiHA and SiHA disks, previously introduced into 24 well culture (CULTEK S.L.U., Madrid, Spain), in Dulbecco´s Modified Eagle´s Medium (DMEM, Sigma Chemical Company, St. Louis, MO, USA) supplemented with 10% (vol/vol) fetal bovine serum (FBS, Gibco, BRL), 1 mM L-glutamine (BioWhittaker Europe, Belgium), penicillin (200 µg/ml, BioWhittaker Europe, Belgium), and streptomycin (200 µg/ml, BioWhittaker Europe, Belgium), under a 5% CO_2 atmosphere and at 37ºC for 24 hours. Then, the medium was aspirated, cells were washed with PBS and harvested using 0.25% trypsin-EDTA solution. For the analysis of cell proliferation, the cell number was calculated with a Neubauer hemocytometer using 10 µl of each cell suspension. Then, cell suspensions were centrifuged at 310xg for 10 min and resuspended in fresh medium for the analysis of different parameters by flow cytometry.

2.4 Early osteoclast-like cell differentiation on nano-SiHA and SiHA disks

Murine RAW-264.7 macrophages ($2x10^4$ cells/ml) were seeded on the surface of nano-SiHA and SiHA disks, previously introduced into 24 well culture (CULTEK S.L.U., Madrid, Spain), in Dulbecco's Modified Eagle Medium (DMEM, Sigma Chemical Company, St. Louis, MO, USA) without phenol red, supplemented with 10% (vol/vol) fetal bovine serum (FBS, Gibco, BRL), 1 mM L-glutamine (BioWhittaker Europe, Belgium), penicillin (200 µg/ml, BioWhittaker Europe, Belgium), and streptomycin (200 µg/ml, BioWhittaker Europe, Belgium). In order to stimulate osteoclast-like cell differentiation, 40 ng/ml of mouse RANK Ligand recombinant protein (TRANCE/RANKL, carrier-free, BioLegend, San Diego) and 25 ng/ml recombinant human macrophage-colony stimulating factor (M-CSF, Milipore, Temecula) were added to the culture medium. Cells were cultured under a 5% CO_2 atmosphere and at 37ºC for 7 days. Then, the medium was aspirated, cells were washed with PBS and harvested using PBS-EDTA during 10 min. For the analysis of cell proliferation, the cell number was calculated with a Neubauer hemocytometer using 10 µl of each cell suspension. Then, cell suspensions were then centrifuged at 310xg for 10 min and resuspended in fresh medium for the analysis of different parameters by flow cytometry.

2.5 Flow Cytometry studies

After incubation with the different probes, as is described below, the conditions for the data acquisition and analysis were established using negative and positive controls with the CellQuest Program of Becton Dickinson. These conditions were maintained during all the experiments. At least 10,000 cells were analyzed in each sample.

2.5.1 Cell cycle analysis and apoptosis detection

Cell suspensions were centrifuged at 310xg for 10 min, resuspended in PBS (0.5 ml) and incubated with 4.5 ml of ethanol 70% during 4 hours at 4ºC. Then, cells were centrifuged at 310xg for 10 min, washed with PBS and resuspended in 0.5 ml of PBS with Tritón X-100 0,1%, IP 20 mg/ml and RNAsa 0,2 mg/ml (Sigma-Aldrich, St. Louis, MO, USA). After incubation at 37ºC for 30 min, the fluorescence of PI was excited by a 15 mW laser tunning to 488 nm and the emitted fluorescence was measured with a 585/42 band pass filter in a FACScalibur Becton Dickinson flow cytometer. The cell percentage in each cycle phase: G0/G1, S and G2/M was calculated with the CellQuest Program of Becton Dickinson and the SubG1 fraction was used as indicative of apoptosis.

2.5.2 Intracellular reactive oxygen species (ROS) content

Cells were incubated at 37ºC for 30 min with 100 μM 2´,7´-dichlorofluorescein diacetate (DCFH/DA, Serva, Heidelberg/Germany) for directly measuring the intracellular content of reactive oxygen species (ROS). DCFH/DA is diffused into cells and is deacetylated by cellular esterases to non-fluorescent DCFH, which is rapidly oxidized to highly fluorescent DCF by ROS. To measure the intracellular ROS content, the DCF fluorescence was excited by a 15 mW laser tuning to 488 nm and the emitted fluorescence was measured with a 530/30 band pass filter in a FACScalibur Becton Dickinson Flow Cytometer.

2.5.3 Cell viability

Cell viability was evaluated by exclusion of propidium iodide (PI; 0.005% wt/vol in PBS, Sigma-Aldrich, St. Louis, MO, USA). PI was added to the cell suspensions in order to stain the DNA of dead cells. The fluorescence of PI was excited by a 15 mW laser tunning to 488 nm and the emitted fluorescence was measured with a 530/30 band pass filter in a FACScalibur Becton Dickinson flow cytometer.

2.6 Morphological studies by Confocal Microscopy

Cells cultured on the surface of nano-SiHA and SiHA disks were fixed with 3.7% paraformaldehyde in PBS for 10 min, washed with PBS and permeabilizated with 0.1% Triton X-100 for 3 to 5 min. The samples were then washed with PBS and preincubated with PBS containing 1% BSA for 20 to 30 min. Then cells were incubated during 20 min with FITC phalloidin (Dilution 1:40, Molecular Probes) to stain F-actin filaments. Samples were then washed with PBS and the cell nuclei were stained with DAPI (4′-6-diamidino-2′-phenylindole, 3 μM in PBS, Molecular Probes). After staining and washing with PBS, cells were examined by a LEICA SP2 Confocal Laser Scanning Microscope. The fluorescence of FITC was excited at 488 nm and the emitted fluorescence was measured at 491-586 nm. DAPI fluorescence was excited at 405 nm and measured at 420–480 nm.

2.7 Morphological Studies by Scanning Electron Microscopy

Cells cultured on the surface of nano-SiHA and SiHA disks were fixed with glutaraldehyde (2.5% in PBS) for 45 min. Sample dehydration was performed by slow water replacement using series of ethanol solutions (30, 50, 70, 90%) for 15 min with a final dehydration in absolute ethanol for 30 min, allowing samples to dry at room temperature and under vacuum. Afterwards, the pieces were mounted on stubs and coated in vacuum with gold-palladium. Cells were examined with a JEOL JSM-6400 LINK IN AN 1000 scanning electron microscope. The chemical composition was obtained by EDX spectroscopy during the surface observation.

2.8 Observation of osteoclast-like cell resorption cavities by Scanning Electron Microscopy

To observe the geometry of resorption cavities produced by osteoclast-like cells on the surface of nano-SiHA and SiHA disks, cells were detached after 7 days culture on these

biomaterials and disks were dehydrated, coated with gold-palladium and examined with a JEOL JSM-6400 scanning electron microscope.

2.9 Statistics

Data are expressed as means + standard deviations of one representative experiment out of three experiments carried out in triplicate. Statistical analysis was performed using the Statistical Package for the Social Sciences (SPSS) version 19 software. Statistical comparisons were made by analysis of variance (ANOVA). Scheffé test was used for post hoc evaluations of differences among groups. In all of the statistical evaluations, $p < 0.05$ was considered as statistically significant.

3. Results and discussion

The success of a biomaterial for bone tissue engineering depends on the bone cell response to its properties at the biomaterial-biological interface. In this context, hydroxyapatite (HA) is widely used because its composition is closest to that of bone mineral (30). Although not highly soluble, HA surfaces can offer nucleating sites for the precipitation of apatite crystals in culture medium (31). Small levels of ionic substitution by silicon in HA have been shown to have significant effects on solubility, bioactivity, osteoclastic and osteoblastic response both *in vitro* and *in vivo* (17,18,24). On the other hand, preparation methods avoiding the high temperature sintering process of hydroxyapatites have been suggested to enhance their bioreactivity, obtaining nanocrystalline bioceramics with higher surface area and smaller crystal size (28,29).

In order to know the nanocrystallinity effects on the response of bone remodelling cells to silicon substituted hydroxyapatite, a comparative *in vitro* study has been carried out with

osteoblasts and osteoclast-like cells cultured on the surface of nanocrystalline (nano-SiHA) and crystalline (SiHA) silicon substituted hydroxyapatite disks.

XRD patterns of nano-SiHA and SiHA (Figure 1a) evidence that both samples are single hydroxyapatite phases. All the diffraction maxima can be assigned to a unique apatite-like phase, indicating that Ca, P and Si got into the hydroxyapatite structure in the amounts stoichiometrically calculated. The broadening of SiHA corresponds with a highly crystalline material as a direct consequence of the high thermal treatment at 1150ºC. The averaged crystallite size calculated for SiHA was 339 nm, as correspond to a highly crystallized ceramic after undergoing a sintering process. On the contrary, nano-SiHA exhibits broader maxima profiles, pointing out that this sample is formed by small crystallites and evidencing that the 700 ºC used in this synthesis could not promote the crystal growth associated with the conventional solid state reaction at higher temperatures. The averaged crystallite size was 32 nm calculated the Rietveld refinement.

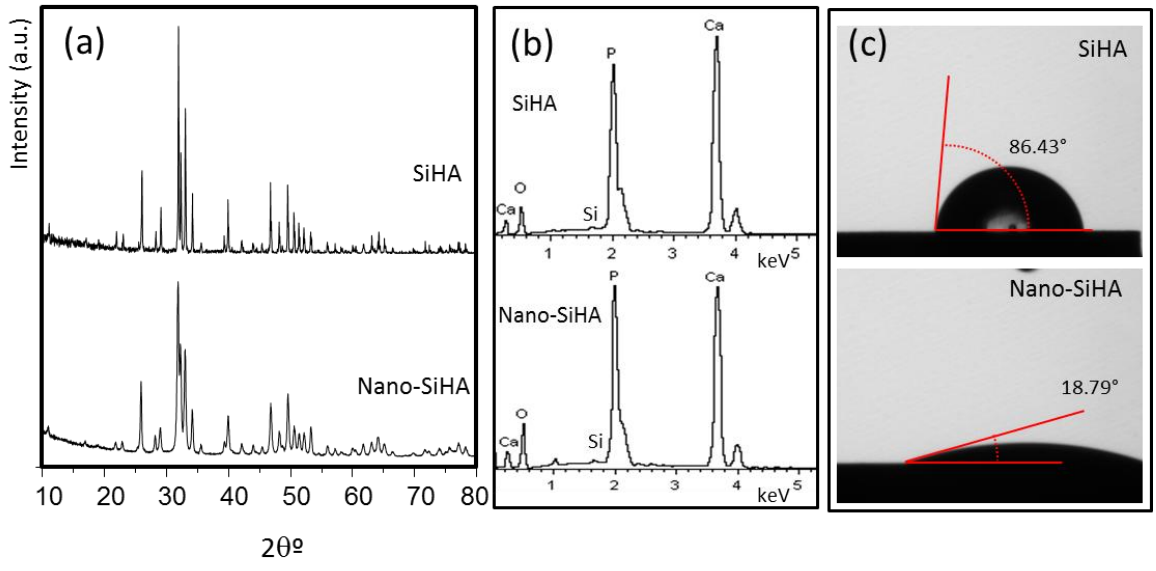

Figure 1. (a) XRD patterns, **(b)** EDX spectra and **(c)** micrographs of a water drop on SiHA and nano-SiHA.

Figure 1.b shows the EDX spectra collected during the SEM observations (see below) indicating that both samples have a very similar surface composition, which corresponds to the constitutive elements for silicon substituted hydroxyapatites, i.e. calcium, phosphorous, oxygen and a small amount of silicon. In order to estimate the wettability of the samples, contact angles measurements were carried out (Figure 1.c). The wettability of the silicon substituted hydroxyapatite significantly decreased with the thermal treatment, which can be explained in terms of a decrease of porosity after the sintering process. The contact angle for nano-SiHA is 18.79º ± 2.95 (indicating a highly hydrophilic surface), whilst that of SiHA is 86.43º ± 0.49.

Table 1 shows the textural parameters and the ζ potential obtained for both nano-SiHA and SiHA. Nano-SiHA exhibits higher surface area and porosity values than those measured for SiHA, which is indicative of a higher number of microstructural defects in this solid. The remaining porosity and insufficient sintering process lead to more reactive surfaces, which not only are more soluble but also more likely to detach particles towards the surrounding media. Moreover, significant differences can be also observed in the ζ potential measurements. Higher thermal treatments seem to shift the surface charge towards more negative values. This fact could play an important role on the biological behavior of both compounds, as it has been described that negative charge values increases the bioactive behavior of calcium phosphate based bioceramics (30). In fact, one of the reasons of the improved bioactivity of silicon substituted respect to non-substituted ones is the extra negative charge introduced by SiO_4^{4-} that substitutes PO_4^{3-}, thus shifting the surface potential towards negative values. In our case, both samples have identical substitution degree and the differences of ζ potential could be due to the presence in nano-SiHA of divalent anions such as CO_3^{2-} or HPO_4^{2-} that can partially remain at 700ºC. After

the thermal treatment at 1150ºC, these anions would be fully substituted by PO_4^{3-} and SiO_4^{4-} thus resulting in more negative potentials at the materials surface.

Table 1. Textural properties and ζ potential of nano-SiHA and Si-HA

Sample	S_{BET} ($m^2 \cdot g^{-1}$)	Pore Volume ($cm^3 \cdot g^{-1}$)	Pore size (nm)	ζ potential (mV)
Nano-SiHA	25.9	0.17	26.8	-8.6
SiHA	1.23	0.003	6.4	-14.5

Figure 2 shows the proliferation values, cell viability and intracellular reactive oxygen species (ROS) content of Saos-2 osteoblasts after 24 h of culture on nano-SiHA and SiHA disks. Although this cell type proliferated on the surface of both biomaterials, the cell number and viability were significantly lower ($p < 0.05$) on nano-SiHA than on SiHA disks. Intracellular ROS levels were also significantly lower in contact with the nanocrystalline material ($p < 0.005$), thus revealing that the nanocrystallinity of SiHA did not induce oxidative stress in this cell type.

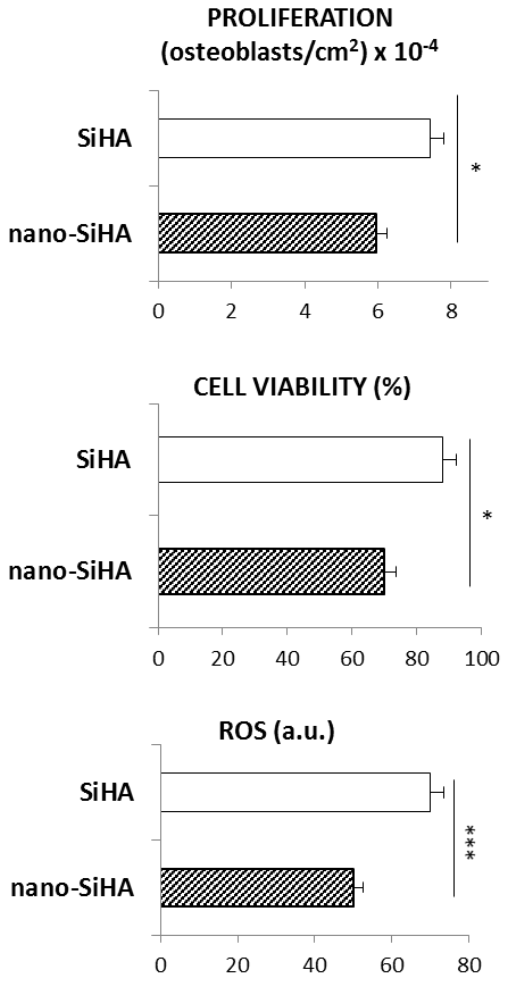

Figure 2. Effects of nano-SiHA and SiHA disks on proliferation, cell viability and intracellular reactive oxygen species (ROS) content of Saos-2 osteoblasts after 24 h of culture. * Comparison between each biomaterial. Statistical significance: *p < 0.05; *** p < 0.005.

In order to know if the decrease produced by nano-SiHA disks on the cell number was due to either cell cycle alterations or apoptosis, the cell cycle phases (G0/G1 = Quiescence/Gap1, S = Synthesis and G2/M = Gap2/Mitosis) of osteoblasts cultured on nano-SiHA and SiHA disks were evaluated by flow cytometry and SubG1 fraction (cells with fragmented DNA) was used as indicative of apoptosis. As it can be observed in Figure 3, the osteoblast SubG1 fraction was significantly higher (p > 0.01) on nano-SiHA disks than on SiHA disks. Nano-SiHA also induced significant decreases of both S (p > 0.05)

and G2/M ($p > 0.01$) phases in comparison with SiHA. These results evidence a slight but significant apoptosis increase and a cell cycle delay in response to the nanocrystalline material. Apoptosis is generally associated with the increase of intracellular reactive oxygen species (ROS) (32), however intracellular ROS levels were significantly lower ($p < 0.005$) in osteoblasts cultured on nano-SiHA than on SiHA disks (Figure 2). The apoptosis increase observed on nano-SiHA could be produced by insufficient and weak contacts between the osteoblasts and the nanocrystalline material surface which can trigger a kind of apoptosis defined as anoikis, induced by the loss of cell/matrix interactions (33-36). This process is important for development and tissue homeostasis, although it has been also related to several diseases (37). The possible loss of cell anchorage due to the nanocrystallinity of nano-SiHA has been also evaluated in the present study by confocal microscopy and scanning electron microscopy.

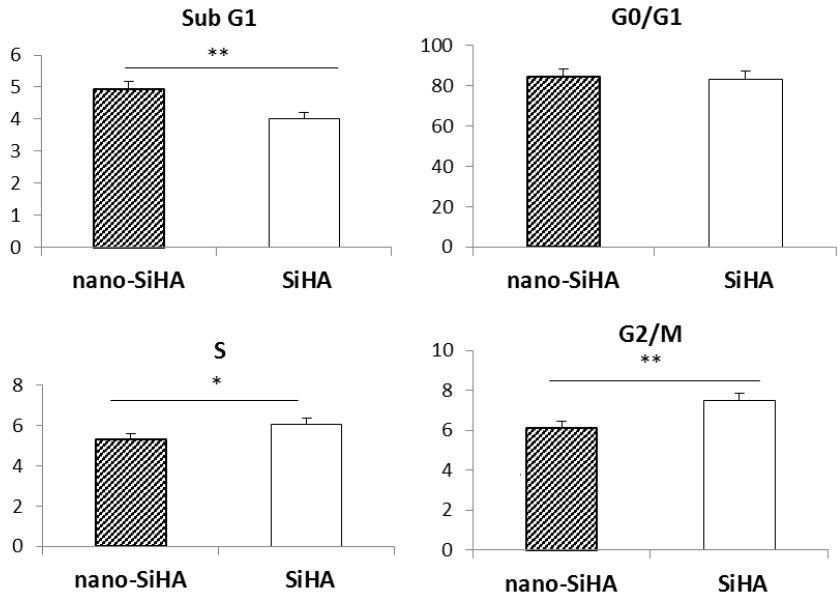

Figure 3. Effects of nano-SiHA and SiHA disks on cell cycle phases of Saos-2 osteoblasts after 24 h of culture. * Comparison between each biomaterial. Statistical significance: *$p < 0.05$; ** $p < 0.01$.

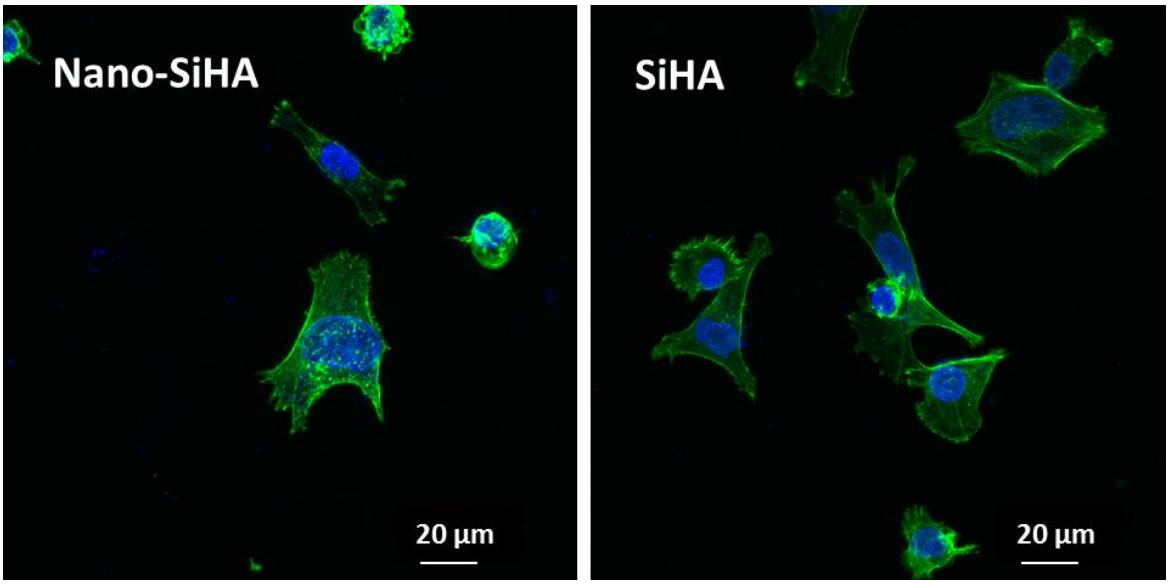

Figure 4. Morphology of Saos-2 osteoblasts on disks of nano-SiHA and SiHA observed by confocal microscopy after 24 h of culture. Actin was stained with FITC-phalloidin (green) and nuclei were stained with DAPI (blue).

Figure 4 shows the morphology of Saos-2 osteoblasts on nano-SiHA and SiHA disks observed by confocal microscopy after 24 h of culture. Actin filaments were stained with FITC-phalloidin (green) and nuclei were stained with DAPI (blue). Osteoblasts were well spread on the disk surface of both hydroxyapatites, with a distinctive actin network and presenting their correct morphology. However the cell number on nano-SiHA disks was lower than on SiHA disks. On the other hand, some cells showing spherical shape with diminished adhesion were observed on nano-SiHA disk surface revealing that the nanocrystalline material could produce anoikis. When Saos-2 osteoblasts cultured on nano-SiHA and SiHA disks were observed by scanning electron microscopy (SEM) after 24 h of culture, SEM images demonstrate the presence of cells attached on both materials, with the typical characteristics of osteoblast morphology (Figure 5). However, these SEM images demonstrate the presence of a higher number of cells attached on SiHA disks than on nano-SiHA, showing long cytoplasmic prolongations to adhere to the surface of SiHA disks. The decrease of the osteoblast number observed by SEM on nano-SiHA, in comparison with SiHA, is in agreement with the proliferation data (Figure 2) and with the confocal

microscopy images (Figure 4). These results indicate a good biocompatibility of both SiHA and nano-SiHA materials but a better interaction of osteoblasts with SiHA disks than with nanocrystalline SiHA disks.

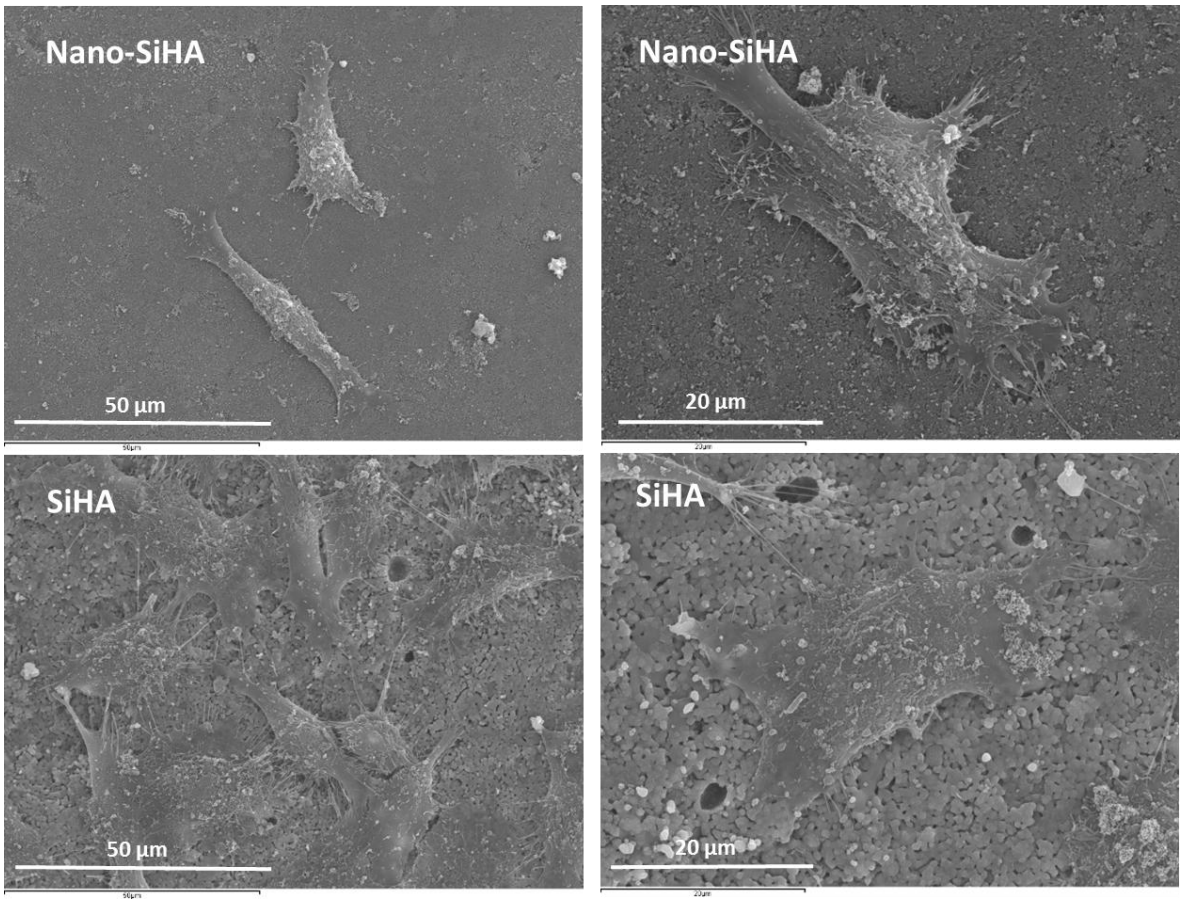

Figure 5. Morphology of Saos-2 osteoblasts on disks of nano-SiHA and SiHA observed by scanning electron microscopy after 24 h of culture.

Previous studies with nanocrystalline hydroxyapatites (nano-SiHA and nano-HA) showed that the substitution with Si delayed the osteoclast-like cell differentiation after 21 days of culture and decreased their resorptive activity without differences in cell viability (38). These results were probably due to the action of Si which can affect the late stages of differentiation and fusion of osteoclasts, causing *in vitro* a significant inhibition of osteoclast phenotypic gene expressions, osteoclast formation and resorptive activity (14). In the present study, in order to know the nanocrystallinity effects of nano-SiHA on the osteoclast differentiation and resorptive activity, murine RAW-264.7 macrophages were

cultured for 7 days on the surface of nanocrystalline (nano-SiHA) and crystalline SiHA disks and differentiated into osteoclast-like cells in the presence of soluble receptor activator of nuclear factor kappa-B ligand (RANKL) and macrophage/monocyte-colony forming factor (M-CSF). The shorter time of 7 days was chosen in order to know the effects of nanocrystallinity of nano-SiHA on the early osteoclast-like cell differentiation, avoiding the effects produced by Si on the late stages of differentiation (14,38).

Figure 6 shows the values of cell proliferation, viability and intracellular reactive oxygen species (ROS) of osteoclast-like cells after 7 days of culture on nano-SiHA and SiHA disks.

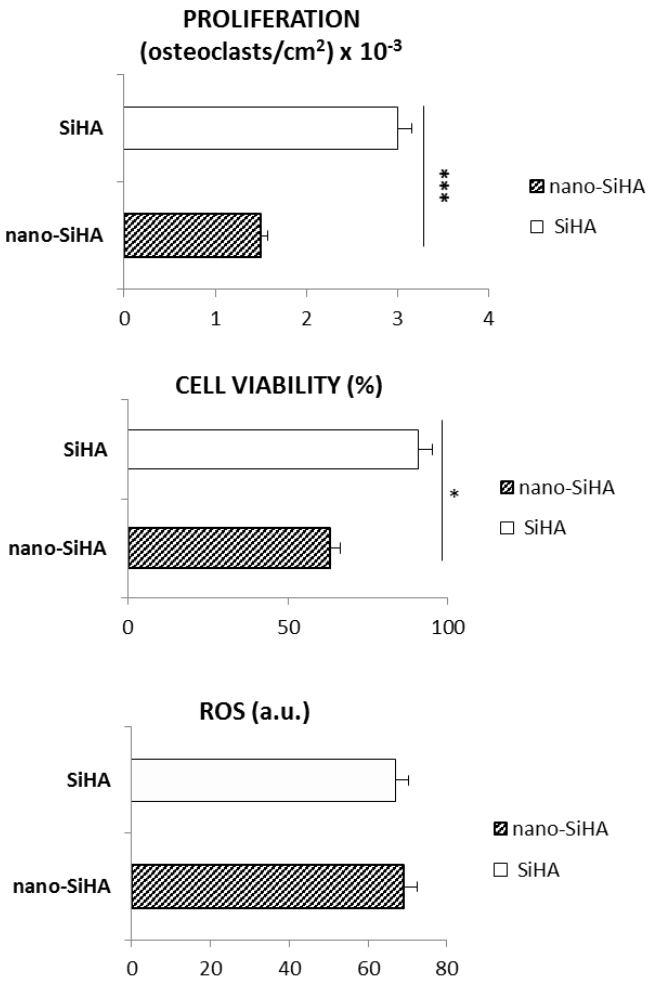

Figure 6. Effects of SiHA and nano-SiHA disks on proliferation, cell viability and intracellular reactive oxygen species (ROS) of osteoclast-like cells after 7 days of culture. * Comparison between each biomaterial. Statistical significance: *$p < 0.05$; *** $p < 0.005$.

The osteoclast-like cell number and viability were significantly lower ($p < 0.005$ and $p < 0.05$ respectively) on nano-SiHA than on SiHA disks. However, intracellular ROS levels were similar on both materials.

The morphology of osteoclast-like cells on disks of nano-SiHA and SiHA was observed by confocal microscopy and SEM after 7 days of culture (Figures 7 and 8 respectively).

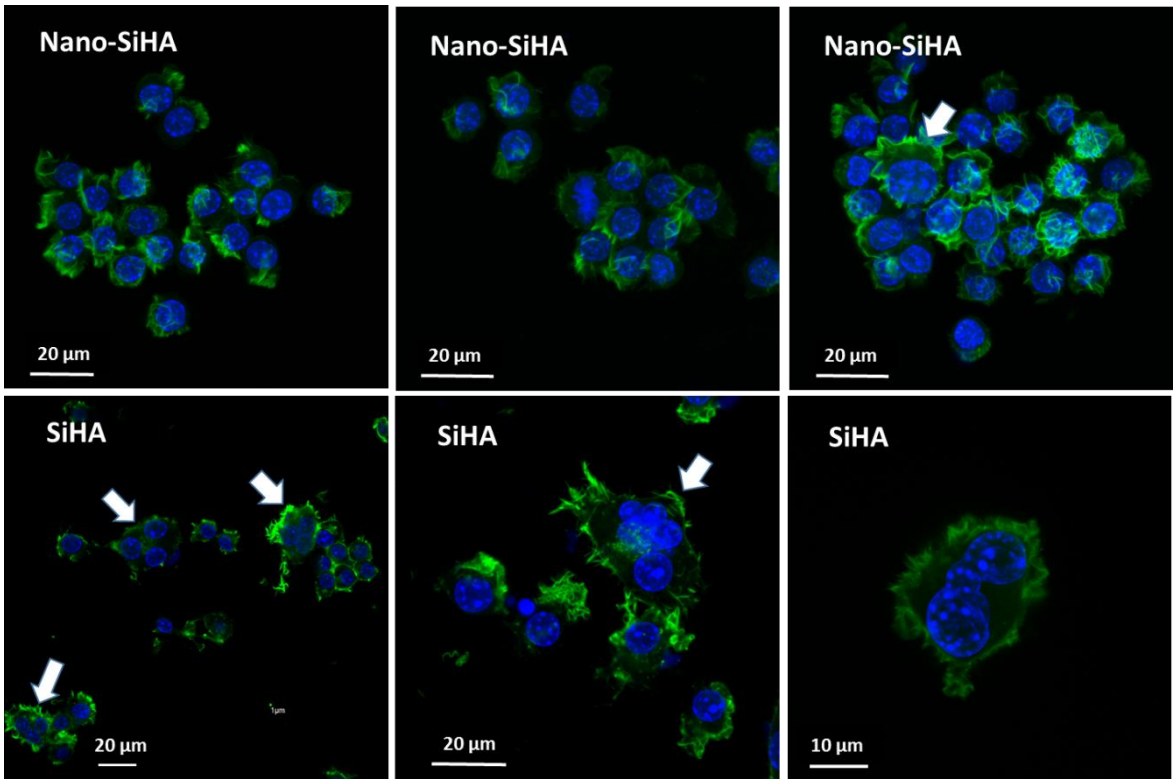

Figure 7. Morphology of osteoclast-like cells on disks of nano-SiHA and SiHA observed by confocal microscopy after 7 days of culture. Actin was stained with FITC-phalloidin (green) and nuclei were stained with DAPI (blue).

Multinucleated cells were observed on SiHA disks (Figure 7, arrows, lower panel) revealing osteoclast-like cell differentiation from RAW macrophages on the surface of this material after 7 days in the presence of RANKL and MSCF. However, multinucleated cells were not obtained on nano-SiHA disks after this treatment (Figure 7, upper panel), thus indicating that the nanocrystalline SiHA induced a delay of the osteoclast differentiation

process in comparison with the crystalline material. The formation of podosomes and the presence of actin rings, which define the sealing zone and are critical for the resorptive activity of this cell type, were also observed on SiHA disks but not on nano-SiHA disks.

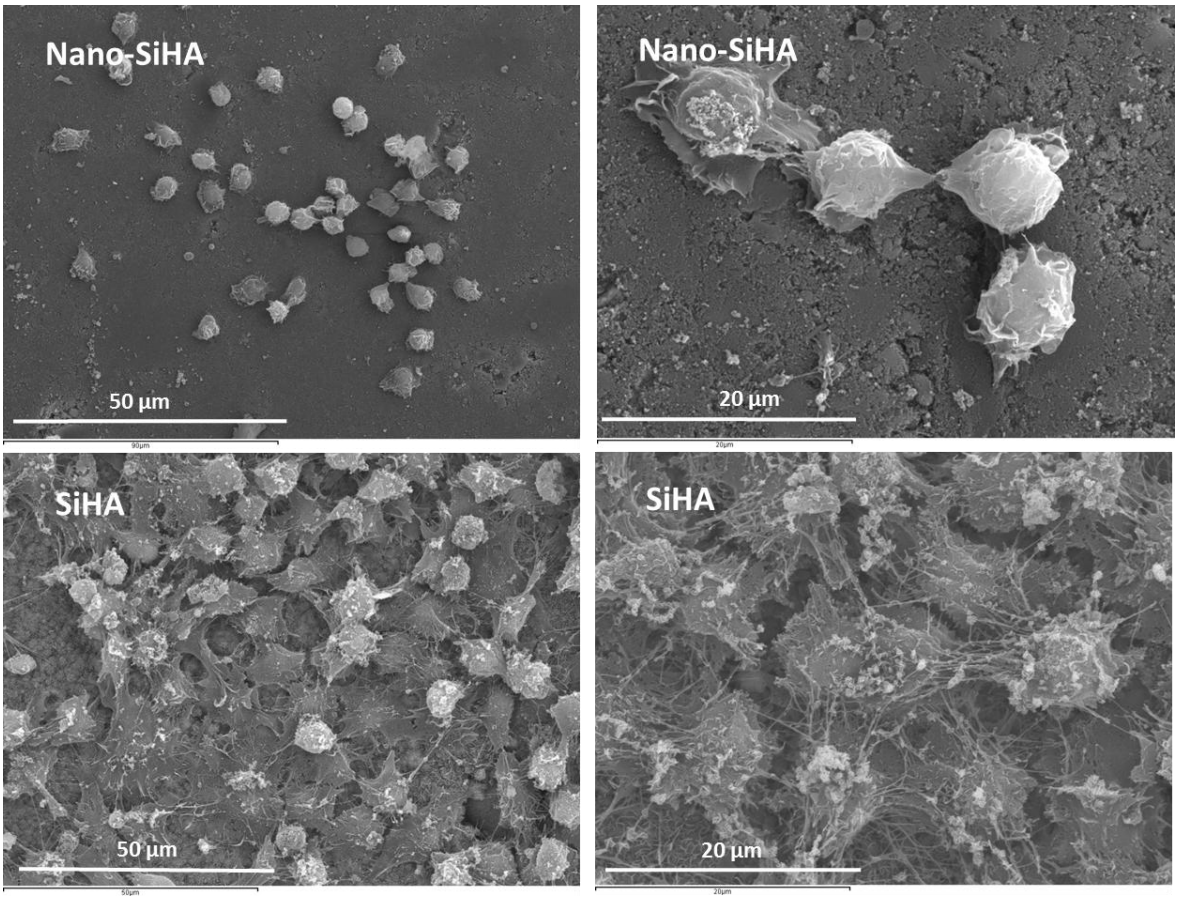

Figure 8. Morphology of osteoclast-like cells on disks of nano-SiHA and SiHA observed by scanning electron mycroscopy after 7 days of culture.

SEM studies showed the presence of a higher number of cells attached on SiHA disks than on nano-SiHA disks (Figure 8). The cells attached on SiHA disks present bigger size than on nano-SiHA disks and the typical characteristics of osteoclast-like cells with many longer podosomes. Cells on nano-SiHA show spherical shape with diminished adhesion which indicates the induction of anoikis by this material. Figure 9 shows the resorption cavities left by osteoclast-like cells cultured on nano-SiHA and SiHA disks after 7 days of

culture evaluated by SEM. The morphology and the number of these cavities evidenced that the resorptive activity were also higher on SiHA disks than on nano-SiHA disks.

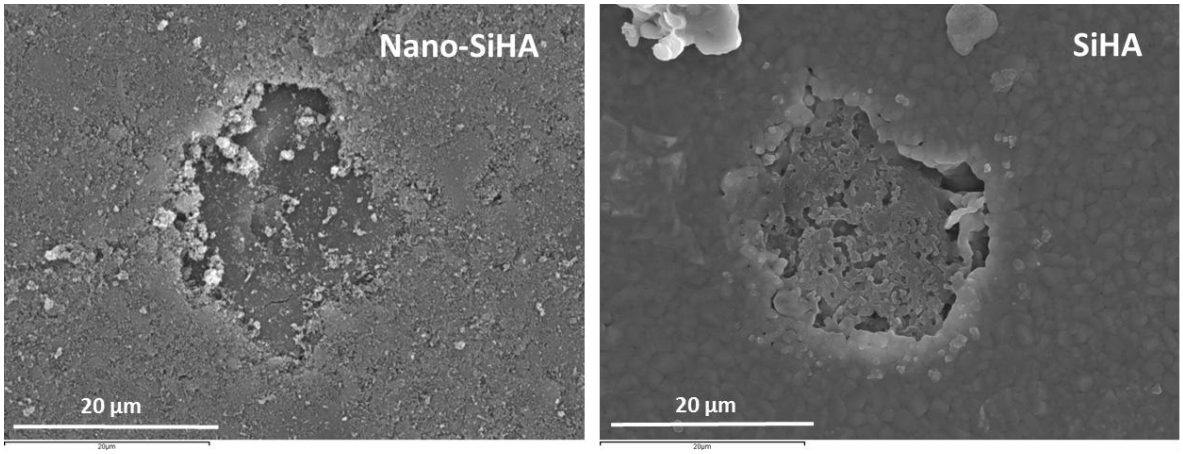

Figure 9. Morphology evaluation by scanning electron microscopy of the resorption cavities left by osteoclast-like cells cultured on nano-SiHA and SiHA disks after 7 days of culture.

All these results demonstrate that the different topography of nanocrystalline SiHA, in comparison with crystalline SiHA, induces anchorage loss of bone cells on its surface, delaying cell adhesion, proliferation, differentiation and activity. Concerning adsorption of serum proteins and fibrinogen, which could be related to the implant success and hemocompatibility, previous studies evidenced that the amount of both serum albumin and fibrinogen adsorbed on crystalline SiHA was significantly lower than on nanocrystalline SiHA (39).

4. Conclusions

Previous studies with nanocrystalline hydroxyapatites (nano-SiHA and nano-HA) showed that the substitution with Si delayed the osteoclast-like cell differentiation after 21 days of culture, decreasing their resorptive activity without affecting cell viability (38), probably due to the Si action on the late stages of differentiation and fusion of osteoclasts (14). In the present work, to know the nanocrystallinity effects of

nano-SiHA on both osteoblasts and osteoclasts, an *in vitro* comparative study between nano-SiHA and crystalline SiHA was carried out after a shorter time (7 days), evidencing that nanocrystallinity of silicon substituted hydroxyapatite affects the bone cell/biomaterial interface inducing bone cell apoptosis by loss of cell anchorage (anoikis), delaying early osteoclast-like cell differentiation and decreasing the resorptive activity of this cell type.

Since osteoclasts, as principal bone-resorbing cells, are involved in the pathogenesis of osteoporosis, these findings are of great interest in relation with the potential use of nanocrystalline silicon substituted hydroxyapatite for preventing bone resorption in treatment of osteoporotic bone. Mineralization studies with an osteopenic sheep model are currently being carried out for *in vivo* evaluation of these hydroxyapatites (project from Ministerio de Economía y Competitividad MAT2013-43299-R) and the obtained results will be included in a future manuscript.

Acknowledgments

This study was supported by research grants from the Ministerio de Ciencia e Innovación (project MAT2012-35556), Ministerio de Economía y Competitividad (project MAT2013-43299-R) and Agening Network of Excellence (CSO2010-11384-E). M.C. Matesanz is greatly indebted to MEC for predoctoral fellowship. The authors wish to thank also to the staff of the ICTS Centro Nacional de Microscopia Electrónica (Spain)) for the assistance in the scanning electron microscopy and to the staff of the Centro de Citometría y Microscopia de Fluorescencia of the Universidad Complutense de Madrid (Spain) for the assistance in the scanning electron microscopy and flow cytometry studies.

References

1. Parfitt AM. Targeted and nontargeted bone remodeling: relationship to basic multicellular unit origination and progression. Bone 2002;30:5-7.

2. Harada S, Rodan GA. Control of osteoblast function and regulation of bone mass. Nature 2003;423:349-55.

3. Mackie EJ. Osteoblasts: novel roles in orchestration of skeletal architecture. Int J Biochem Cell Biol 2003;35:1301-5.

4. Boyle WJ, Simonet WS, Lacey DL. Osteoclast differentiation and activation. Nature 2003;423:337-42.

5. Qin A, Cheng TS, Pavlos NJ, Lin Z, Dai KR, Zheng MH. V-ATPases in osteoclasts: structure, function and potential inhibitors of bone resorption. Int J Biochem Cell Biol 2012;44:1422-35.

6. Väänänen HK, Liu YK, Lehenkari P, Uemara T. How do osteoclasts resorb bone?. Mater Sci Eng C 1998;6:205-9.

7. Manolagas SC. Cellular and molecular mechanisms of osteoporosis. Aging 1988;10:182-90.

8. Luhmann T, Germershaus O, Groll J, Meinel L. Bone targeting for the treatment of osteoporosis. J Control Release 2012;161:198-213.

9. Carlisle EM. Silicon as a trace nutrient. Sci Total Environ 1998;73:95-106.

10. Schwarz K. A bound form of silicon in glycosaminoglycans and polyuronides. Proc Natl Acad Sci 1973;70:1608-12.

11. Carlisle EM. *In vivo* requirement for silicon in articular cartilage and connective tissue formation in the chick. J Nutr 1976;106:478-84.

12. Landis WJ, Lee DD, Brenna JT, Chandra S, Morrison GH. Detection and localization of silicon and associated elements in vertebrate bone tissue by imaging ion microscopy. Calcif Tissue Int 1986;38:52-9.

13. Reffitt DM, Ogston DN, Jugdaohsingh R, Cheung HF, Evans BA, Thompson RF, Powell JJ, Hampson GN. Orthosilicic acid stimulates collagen type 1 synthesis and osteoblastic differentiation in human osteoblast-like cells *in vitro*. Bone 2003;32:127-35.

14. Mladenović Z, Johansson A, Willman B, Shahabi K, Björn E, Ransjö M. Soluble silica inhibits osteoclast formation and bone resorption *in vitro*. Acta Biomater 2014;10:406-18.

15. Li H, Chang J. Bioactive silicate materials stimulate angiogenesis in fibroblast and endothelial cell co-culture system through paracrine effect. Acta Biomater 2013;9:6981-91.

16. Bouletreau PJ, Warren SM, Spector JA, Peled ZM, Gerrets RP, Greenwald JA, Longaker MT. Hypoxia and VEGF up-regulate BMP-2 mRNA and protein expression in microvascular endothelial cells: implications for fracture healing. Plast Reconstr Surg 2002;109:2384-97.

17. Shepherd JH, Shepherd DV, Best SM. Substituted hydroxyapatites for bone repair. J Mater Sci Mater Med 2012;23:2335-47.

18. Patel N, Best SM, Bonfield W, Gibson IR, Hing KA, Damien E, Revell PA. A comparative study on the *in vivo* behavior of hydroxyapatite and silicon substituted hydroxyapatite granules. J Mater Sci Mater Med 2002;13:1199-206.

19. Pietak AM, Reid JW, Stott MJ, Sayer M. Silicon substitution in the calcium phosphate bioceramics. Biomaterials 2007;28:4023-32.

20. Bohner M. Silicon-substituted calcium phosphates - a critical view. Biomaterials 2009;30:6403-6.

21. Balas F, Pérez-Pariente J, Vallet-Regí M. *In vitro* bioactivity of silicon-substituted hydroxyapatites. J Biomed Mater Res A 2003;66:364-75.

22. Porter AE, Best SM, Bonfield W. Ultrastructural comparison of hydroxyapatite and silicon-substituted hydroxyapatite for biomedical applications. J Biomed Mater Res A 2004;68:133-41.

23. Dvorak MM, Siddiqua A, Ward DT, Carter DH, Dallas SL, Nemeth EF, Riccardi D. Physiological changes in extracellular calcium concentration directly control osteoblast function in the absence of calciotropic hormones. Proc Natl Acad Sci 2004;101:5140-5.

24. Porter AE, Patel N, Skepper JN, Best SM, Bonfield W. Comparison of *in vivo* dissolution processes in hydroxyapatite and silicon-substituted hydroxyapatite bioceramics. Biomaterials 2003;24:4609-20.

25. Matesanz MC, Feito MJ, Ramírez-Santillán C, Lozano RM, Sánchez-Salcedo S, Arcos D, Vallet-Regí M, Portolés MT. Signaling pathways of immobilized FGF-2 on silicon-substituted hydroxyapatite. Macromol Biosci 2012;12:446-53.

26. Balamurugan A, Rebelo AHS, Lemos AF, Rocha JHG, Ventura JMG, Ferreira JMF. Suitability evaluation of sol-gel derived Si-substituted hydroxyapatite for dental and maxillofacial applications through in vitro osteoblasts response. Dent Mater 2008;24:1374-80.

27. Arcos D, Rodríguez-Carvajal J, Vallet-Regí M. Silicon incorporation in hydroxylapatite obtained by controlled crystallization. Chem Mater 2004;16:2300-8.

28. Dorozhkin SV. Nanodimensional and nanocrystalline apatites and other calcium orthophosphates in Biomedical Engineering, Biology and Medicine. Materials 2009;2:1975-2045.

29. Thian ES, Ahmad Z, Huang J, Edirisinghe MJ, Jayasinghe SN, Ireland DC, Brooks RA, Rushton N, Bonfield W, Best SM. The role of surface wettability and surface charge of electrosprayed nanoapatites on the behaviour of osteoblasts. Acta Biomater 2010;6:750-5.

30. Samaved S, Whittington AR, Goldstein AS. Calcium phosphate ceramics in bone tissue engineering: a review of properties and their influence on cell behavior. Acta Biomater 2013;9:8037-45.

31. Bohner M, Lemaitre J. Can bioactivity be tested *in vitro* with SBF solution?. Biomaterials 2009;30:2175-9.

32. Quillet-Mary A, Jaffrezou JP, Mansat V, Bordier C, Naval J, Laurent G. Implication of mitochondrial hydrogen peroxide generation in ceramide-induced apoptosis. J Biol Chem 1997;272:21388-95.

33. Frisch SM, Ruoslaht E. Integrins and anoikis. Curr Opin Cell Biol 1997;9:701-6.

34. Frisch SM, Screaton RA. Anoikis mechanisms. Curr Opin Cell Biol 2001;13:555-62.

35. Grossmann J, Walther K, Artinger M, Kiessling S, Scholmerich J. Apoptotic signaling during initiation of detachment-induced apoptosis ("anoikis") of primary human intestinal epithelial cells. Cell Growth Differ 2001;12:147-55.

36. Alcaide M, Serrano MC, Román J, Cabañas MV, Peña J, Sánchez-Zapardiel E, Vallet-Regí M, Portolés MT. Suppression of anoikis by collagen coating of interconnected macroporous nanometric carbonated hydroxyapatite/agarose scaffolds. J Biomed Mater Res A 2010;95:793-800.

37. Chiarugi P, Giannoni E. Anoikis: a necessary death program for anchorage-dependent cells. Biochem Pharmacol 2008;76:1352-64.

38. Matesanz MC, Linares J, Lilue I, Sánchez-Salcedo S, Feito MJ, Arcos D, Vallet-Regí M, Portolés MT. Nanocrystalline silicon substituted hydroxyapatite effects on osteoclast differentiation and resorptive activity. J Mater Chem B 2014;2:2910-9.

39. Matesanz MC, Linares J, Oñaderra M, Feito MJ, Martínez-Vázquez FJ, Sánchez-Salcedo S, Arcos D, Portolés MT, Vallet-Regí M. Response of osteoblasts and preosteoblasts to calcium deficient and Si substituted hydroxyapatites treated at different temperatures. Colloids Surf, B 2015;133:304-13.

Nanocrystallinity effects on osteoblast and osteoclast response to silicon substituted hydroxyapatite

Laura Casarrubios [a,b], María Concepción Matesanz [a], Sandra Sánchez-Salcedo [c,d], Daniel Arcos [c,d], María Vallet-Regí [c,d], María Teresa Portolés [a,b,*]

[a] Department of Biochemistry and Molecular Biology I/Faculty of Chemistry, Universidad Complutense de Madrid, Spain
[b] Instituto de Investigación Sanitaria San Carlos IdISSC, Spain
portoles@quim.ucm.es, arualanilom@hotmail.com, conchitamatesanz@hotmail.com

[c] Department of Inorganic and Bioinorganic Chemistry/Faculty of Pharmacy, Universidad Complutense de Madrid, Instituto de Investigación Hospital 12 de Octubre i+12, Spain
[d] Networking Research Center on Bioengineering/Biomaterials and Nanomedicine, CIBER-BBN, Spain
vallet@ucm.es, arcosd@ucm.es, sansanch@ucm.es

* Corresponding author: María Teresa Portolés.
E-mail address: portoles@quim.ucm.es

Abstract

Hypothesis: Silicon substituted hydroxyapatites (SiHA) are highly crystalline bioceramics treated at high temperatures (about 1200ºC) which have been approved for clinical use with spinal, orthopedic, periodontal, oral and craniomaxillofacial applications. The preparation of SiHA with lower temperature methods (about 700ºC) provides nanocrystalline SiHA (nano-SiHA) with enhanced bioreactivity due to higher surface area and smaller crystal size. The aim of this study has been to know the nanocrystallinity effects on the response of both osteoblasts and osteoclasts (the two main cell types involved in bone remodelling) to silicon substituted hydroxyapatite.

Experiments: Saos-2 osteoblasts and osteoclast-like cells (differentiated from RAW-264.7 macrophages) have been cultured on the surface of nano-SiHA and SiHA disks and different cell parameters have been evaluated: cell adhesion, proliferation, viability, intracellular content of reactive oxygen species, cell cycle phases, apoptosis, cell morphology, osteoclast-like cell differentiation and resorptive activity.

Findings: This comparative *in vitro* study evidences that nanocrystallinity of SiHA affects the cell/biomaterial interface inducing bone cell apoptosis by loss of cell anchorage (anoikis), delaying osteoclast-like cell differentiation and decreasing the resorptive activity of this cell type. These results suggest the potential use of nano-SiHA biomaterial for preventing bone resorption in treatment of osteoporotic bone.

Keywords: nanocrystallinity, hydroxyapatite, silicon, osteoclast, osteoblast, anoikis, osteoporosis, cell adhesion, apoptosis, cell cycle.

1. Introduction

Bone is a metabolically active and very dynamic tissue in continuous resorption and formation by osteoclasts and osteoblasts respectively, working together via paracrine cell signaling in basic multicellular units (1). Osteoblasts are mononucleated cells which differentiate from mesenchymal stem cells of the bone marrow stroma and are responsible for deposition of bone matrix and regulation of osteoclasts (2,3). Osteoclasts are multinucleated giant cells which differentiate from hematopoietic stem cells (that give rise to monocytes and macrophages) and they perform the bone resorption (4). Osteoclasts attach to the bone surface and initiate resorption by the secretion of hydrogen ions and lysosomal enzymes which degrade all the components of bone matrix producing irregular cavities on the bone surface (5,6). The balance between bone resorption by osteoclasts and bone formation by osteoblasts is influenced by mechanical, genetic, vascular, nutritional, hormonal and local factors. This bone remodeling is necessary to maintain the structural skeleton integrity and mineral homeostasis. Alterations of this process are involved in the pathogenesis of various skeletal diseases, including osteoporosis (7,8).

Silicon (Si) is an essential element for bone and cartilage formation (9-11) and is present in the areas of greatest osteoblastic activity during bone growth (12). This element is essential to the normal development of the glycosaminoglycan network in the extracellular matrix (9), increasing bone collagen content (13). Si also appears to inhibit macrophage and osteoclast activity (14). Bioactive silicate materials upregulate the expression of vascular endothelial growth factor (VEGF) (15), which is involved in both blood vessel and bone formation (16). Small levels of ionic substitution by Si in hydroxyapatite (HA) have been shown to have significant effects on thermal stability, solubility, osteoclastic and osteoblastic response both *in vitro* and *in vivo* (17). Thus, silicon substituted

hydroxyapatite (SiHA) presents enhanced bioactivity *in vivo* than HA, showing beneficial effects in the early stages of bone formation (18). The favourable effects of Si substitution in HA have been explained by considering passive and active mechanisms as material solubility increase, topographical changes, grain size reduction, surface charge modifications and ionic release of Si and Ca, which directly act on bone cells (19-23). All these facts make SiHA very attractive for use as bone substitute material (24-27) and SiHA has recently been incorporated to the biomaterials market as Actifuse ABXTM (Apatech Ltd, UK) for spinal, orthopedic, periodontal, oral and craniomaxillofacial applications. SiHA approved for clinical use are highly crystalline bioceramics treated at high temperatures (about 1200ºC). However, their preparation with lower temperature methods has been suggested to enhance the bioreactivity of these bioceramics (28-30). Avoiding the high temperature sintering process, nanocrystalline pieces and grains can be prepared with higher surface area and smaller crystal size. These characteristics could provide very interesting bioresponses in SiHA since the osteogenic effect of silicon is mainly explained by its location at the crystal boundaries (24,25).

The novelty of the present study is the comparison of the action of nanocrystalline and crystalline silicon substituted hydroxyapatites (nano-SiHA and SiHA respectively) on both osteoblasts and osteoclasts, the two main cell types involved in bone remodelling. In this comparative *in vitro* study, Saos-2 osteoblasts and osteoclast-like cells (differentiated from RAW-264.7 macrophages) have been cultured on the surface of nano-SiHA and SiHA disks and different cell parameters have been evaluated: cell adhesion, proliferation, viability, intracellular content of reactive oxygen species (ROS), cell cycle phases, apoptosis, cell morphology, osteoclast-like cell differentiation and resorptive activity.

2. Materials and methods

2.1 *Synthesis of materials*

Silicon-substituted hydroxyapatite (Si-HA) with nominal formula $Ca_{10}(PO_4)_{5.75}(SiO_4)_{0.25}(OH)_{1.75}\square_{0.25}$, where □ means vacancies at the hydroxyl position, was prepared by aqueous precipitation reaction of $Ca(NO_3)_2{\cdot}4H_2O$, $(NH_4)_2HPO_4$ and $Si(CH_3CH_2O)_4$ solutions. Briefly, a 1 M solution of $Ca(NO_3)_2{\cdot}4H_2O$ was added to a second 0.575 M of $(NH_4)_2HPO_4$ and 0,025 M of $Si(CH_3CH_2O)_4$ solution to obtain the composition described above. The mixture was stirred for 12 h at 80°C. The pH was kept at 9.5 by NH_3 solution addition to ensure constant conditions during the synthesis. The precipitated Si-HA powder was dried, milled and sieved and the powder fraction below 40 μm was selected. Fractions of 300 mg of powder were pressed into disk-shape (11 mm diameter, 2 mm height) by means of 3 tons of uniaxial pressing. Subsequently the discs were treated during 3 hours at 700ºC or 1150ºC resulting in nano-SiHA or SiHA, respectively.

2.2 Characterization of materials

The structural characterization was performed by Powder X-ray diffraction (XRD) in a Philips X'Pert diffractometer equipped with a CuKα radiation (wavelength 1.5406 Å), with a step size of 0.02º 2θ and 8 seconds of counting time. In order to determine the crystalline and microstructural characteristics of both samples, Rietveld refinements were carried out over the XRD patterns collected. The refinements were performed using the atomic position set and the space group of the HA structure P63/m, No. 176 by means of the FullProf 2000 computer program. The instrumental resolution function (IRF) of the diffractometer was obtained from a very-well-crystallized LaB_6 sample and taken into

account in a separate input file. The pseudo-Voigt profile function of Thompson, Cox, and Hastings was used with an asymmetry correction at a low angle.

The contact angles were measured to estimate the wettability of the samples. The experiments were performed by the sessile drop method at 25º C on a CAM 200 KSV contact angle goniometer. Pictures of the drops were taken every 1 s. The software delivered by the instrument manufacturer calculated the contact angles on the basis of a numerical solution of the full Young–Laplace equation.

Textural properties (surface and porosity) were determined by nitrogen adsorption porosimetry in a Micromeritics ASAP 2012. To perform the N_2 adsorption measurements, the samples were previously degassed under vacuum for 24 h at 80ºC. Finally, zeta potential was measured by means of a Zetasizer Nano ZS (Malvern Instruments).

2.3 Culture of osteoblasts in contact with nano-SiHA and SiHA

Human Saos-2 osteoblasts (10^5 cells/ml) were seeded on the surface of nano-SiHA and SiHA disks, previously introduced into 24 well culture (CULTEK S.L.U., Madrid, Spain), in Dulbecco´s Modified Eagle´s Medium (DMEM, Sigma Chemical Company, St. Louis, MO, USA) supplemented with 10% (vol/vol) fetal bovine serum (FBS, Gibco, BRL), 1 mM L-glutamine (BioWhittaker Europe, Belgium), penicillin (200 µg/ml, BioWhittaker Europe, Belgium), and streptomycin (200 µg/ml, BioWhittaker Europe, Belgium), under a 5% CO_2 atmosphere and at 37ºC for 24 hours. Then, the medium was aspirated, cells were washed with PBS and harvested using 0.25% trypsin-EDTA solution. For the analysis of cell proliferation, the cell number was calculated with a Neubauer hemocytometer using 10 µl of each cell suspension. Then, cell suspensions were centrifuged at 310xg for 10 min and resuspended in fresh medium for the analysis of different parameters by flow cytometry.

2.4 Early osteoclast-like cell differentiation on nano-SiHA and SiHA disks

Murine RAW-264.7 macrophages ($2x10^4$ cells/ml) were seeded on the surface of nano-SiHA and SiHA disks, previously introduced into 24 well culture (CULTEK S.L.U., Madrid, Spain), in Dulbecco's Modified Eagle Medium (DMEM, Sigma Chemical Company, St. Louis, MO, USA) without phenol red, supplemented with 10% (vol/vol) fetal bovine serum (FBS, Gibco, BRL), 1 mM L-glutamine (BioWhittaker Europe, Belgium), penicillin (200 µg/ml, BioWhittaker Europe, Belgium), and streptomycin (200 µg/ml, BioWhittaker Europe, Belgium). In order to stimulate osteoclast-like cell differentiation, 40 ng/ml of mouse RANK Ligand recombinant protein (TRANCE/RANKL, carrier-free, BioLegend, San Diego) and 25 ng/ml recombinant human macrophage-colony stimulating factor (M-CSF, Milipore, Temecula) were added to the culture medium. Cells were cultured under a 5% CO_2 atmosphere and at 37ºC for 7 days. Then, the medium was aspirated, cells were washed with PBS and harvested using PBS-EDTA during 10 min. For the analysis of cell proliferation, the cell number was calculated with a Neubauer hemocytometer using 10 µl of each cell suspension. Then, cell suspensions were then centrifuged at 310xg for 10 min and resuspended in fresh medium for the analysis of different parameters by flow cytometry.

2.5 Flow Cytometry studies

After incubation with the different probes, as is described below, the conditions for the data acquisition and analysis were established using negative and positive controls with the CellQuest Program of Becton Dickinson. These conditions were maintained during all the experiments. At least 10,000 cells were analyzed in each sample.

2.5.1 Cell cycle analysis and apoptosis detection

Cell suspensions were centrifuged at 310xg for 10 min, resuspended in PBS (0.5 ml) and incubated with 4.5 ml of ethanol 70% during 4 hours at 4ºC. Then, cells were centrifuged at 310xg for 10 min, washed with PBS and resuspended in 0.5 ml of PBS with Tritón X-100 0,1%, IP 20 mg/ml and RNAsa 0,2 mg/ml (Sigma-Aldrich, St. Louis, MO, USA). After incubation at 37ºC for 30 min, the fluorescence of PI was excited by a 15 mW laser tunning to 488 nm and the emitted fluorescence was measured with a 585/42 band pass filter in a FACScalibur Becton Dickinson flow cytometer. The cell percentage in each cycle phase: G0/G1, S and G2/M was calculated with the CellQuest Program of Becton Dickinson and the SubG1 fraction was used as indicative of apoptosis.

2.5.2 Intracellular reactive oxygen species (ROS) content

Cells were incubated at 37ºC for 30 min with 100 μM 2´,7´-dichlorofluorescein diacetate (DCFH/DA, Serva, Heidelberg/Germany) for directly measuring the intracellular content of reactive oxygen species (ROS). DCFH/DA is diffused into cells and is deacetylated by cellular esterases to non-fluorescent DCFH, which is rapidly oxidized to highly fluorescent DCF by ROS. To measure the intracellular ROS content, the DCF fluorescence was excited by a 15 mW laser tuning to 488 nm and the emitted fluorescence was measured with a 530/30 band pass filter in a FACScalibur Becton Dickinson Flow Cytometer.

2.5.3 Cell viability

Cell viability was evaluated by exclusion of propidium iodide (PI; 0.005% wt/vol in PBS, Sigma-Aldrich, St. Louis, MO, USA). PI was added to the cell suspensions in order to stain the DNA of dead cells. The fluorescence of PI was excited by a 15 mW laser tunning to 488 nm and the emitted fluorescence was measured with a 530/30 band pass filter in a FACScalibur Becton Dickinson flow cytometer.

2.6 Morphological studies by Confocal Microscopy

Cells cultured on the surface of nano-SiHA and SiHA disks were fixed with 3.7% paraformaldehyde in PBS for 10 min, washed with PBS and permeabilizated with 0.1% Triton X-100 for 3 to 5 min. The samples were then washed with PBS and preincubated with PBS containing 1% BSA for 20 to 30 min. Then cells were incubated during 20 min with FITC phalloidin (Dilution 1:40, Molecular Probes) to stain F-actin filaments. Samples were then washed with PBS and the cell nuclei were stained with DAPI (4′-6-diamidino-2′-phenylindole, 3 μM in PBS, Molecular Probes). After staining and washing with PBS, cells were examined by a LEICA SP2 Confocal Laser Scanning Microscope. The fluorescence of FITC was excited at 488 nm and the emitted fluorescence was measured at 491-586 nm. DAPI fluorescence was excited at 405 nm and measured at 420–480 nm.

2.7 Morphological Studies by Scanning Electron Microscopy

Cells cultured on the surface of nano-SiHA and SiHA disks were fixed with glutaraldehyde (2.5% in PBS) for 45 min. Sample dehydration was performed by slow water replacement using series of ethanol solutions (30, 50, 70, 90%) for 15 min with a final dehydration in absolute ethanol for 30 min, allowing samples to dry at room temperature and under vacuum. Afterwards, the pieces were mounted on stubs and coated in vacuum with gold-palladium. Cells were examined with a JEOL JSM-6400 LINK IN AN 1000 scanning electron microscope. The chemical composition was obtained by EDX spectroscopy during the surface observation.

2.8 Observation of osteoclast-like cell resorption cavities by Scanning Electron Microscopy

To observe the geometry of resorption cavities produced by osteoclast-like cells on the surface of nano-SiHA and SiHA disks, cells were detached after 7 days culture on these

biomaterials and disks were dehydrated, coated with gold-palladium and examined with a JEOL JSM-6400 scanning electron microscope.

2.9 Statistics

Data are expressed as means + standard deviations of one representative experiment out of three experiments carried out in triplicate. Statistical analysis was performed using the Statistical Package for the Social Sciences (SPSS) version 19 software. Statistical comparisons were made by analysis of variance (ANOVA). Scheffé test was used for post hoc evaluations of differences among groups. In all of the statistical evaluations, $p < 0.05$ was considered as statistically significant.

3. Results and discussion

The success of a biomaterial for bone tissue engineering depends on the bone cell response to its properties at the biomaterial-biological interface. In this context, hydroxyapatite (HA) is widely used because its composition is closest to that of bone mineral (30). Although not highly soluble, HA surfaces can offer nucleating sites for the precipitation of apatite crystals in culture medium (31). Small levels of ionic substitution by silicon in HA have been shown to have significant effects on solubility, bioactivity, osteoclastic and osteoblastic response both *in vitro* and *in vivo* (17,18,24). On the other hand, preparation methods avoiding the high temperature sintering process of hydroxyapatites have been suggested to enhance their bioreactivity, obtaining nanocrystalline bioceramics with higher surface area and smaller crystal size (28,29).

In order to know the nanocrystallinity effects on the response of bone remodelling cells to silicon substituted hydroxyapatite, a comparative *in vitro* study has been carried out with

osteoblasts and osteoclast-like cells cultured on the surface of nanocrystalline (nano-SiHA) and crystalline (SiHA) silicon substituted hydroxyapatite disks.

XRD patterns of nano-SiHA and SiHA (Figure 1a) evidence that both samples are single hydroxyapatite phases. All the diffraction maxima can be assigned to a unique apatite-like phase, indicating that Ca, P and Si got into the hydroxyapatite structure in the amounts stoichiometrically calculated. The broadening of SiHA corresponds with a highly crystalline material as a direct consequence of the high thermal treatment at 1150ºC. The averaged crystallite size calculated for SiHA was 339 nm, as correspond to a highly crystallized ceramic after undergoing a sintering process. On the contrary, nano-SiHA exhibits broader maxima profiles, pointing out that this sample is formed by small crystallites and evidencing that the 700 ºC used in this synthesis could not promote the crystal growth associated with the conventional solid state reaction at higher temperatures. The averaged crystallite size was 32 nm calculated the Rietveld refinement.

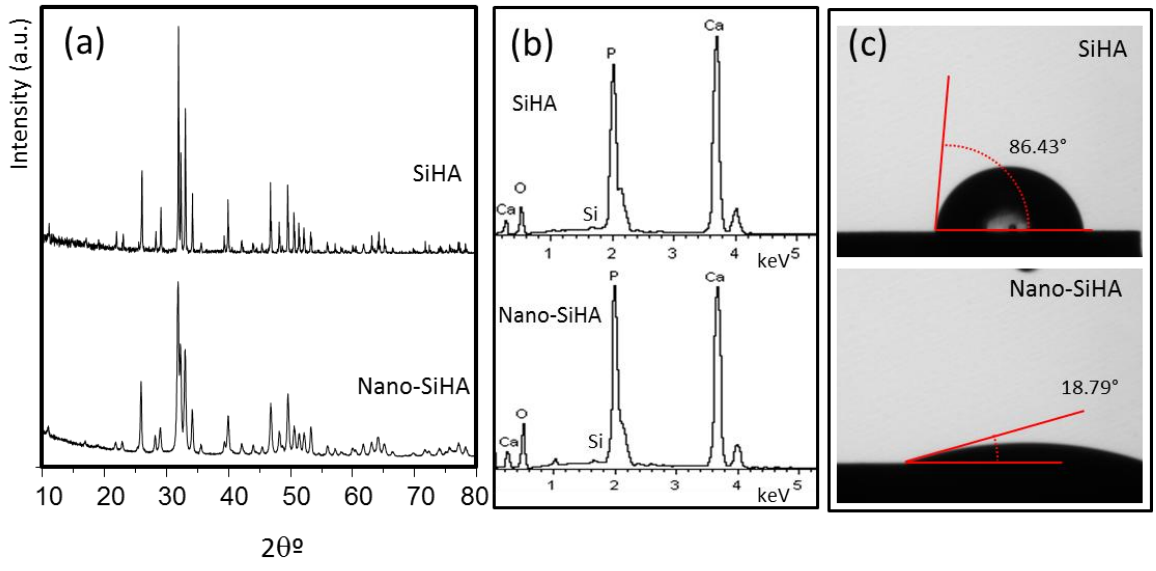

Figure 1. (a) XRD patterns, **(b)** EDX spectra and **(c)** micrographs of a water drop on SiHA and nano-SiHA.

Figure 1.b shows the EDX spectra collected during the SEM observations (see below) indicating that both samples have a very similar surface composition, which corresponds to the constitutive elements for silicon substituted hydroxyapatites, i.e. calcium, phosphorous, oxygen and a small amount of silicon. In order to estimate the wettability of the samples, contact angles measurements were carried out (Figure 1.c). The wettability of the silicon substituted hydroxyapatite significantly decreased with the thermal treatment, which can be explained in terms of a decrease of porosity after the sintering process. The contact angle for nano-SiHA is 18.79º ± 2.95 (indicating a highly hydrophilic surface), whilst that of SiHA is 86.43º ± 0.49.

Table 1 shows the textural parameters and the ζ potential obtained for both nano-SiHA and SiHA. Nano-SiHA exhibits higher surface area and porosity values than those measured for SiHA, which is indicative of a higher number of microstructural defects in this solid. The remaining porosity and insufficient sintering process lead to more reactive surfaces, which not only are more soluble but also more likely to detach particles towards the surrounding media. Moreover, significant differences can be also observed in the ζ potential measurements. Higher thermal treatments seem to shift the surface charge towards more negative values. This fact could play an important role on the biological behavior of both compounds, as it has been described that negative charge values increases the bioactive behavior of calcium phosphate based bioceramics (30). In fact, one of the reasons of the improved bioactivity of silicon substituted respect to non-substituted ones is the extra negative charge introduced by SiO_4^{4-} that substitutes PO_4^{3-}, thus shifting the surface potential towards negative values. In our case, both samples have identical substitution degree and the differences of ζ potential could be due to the presence in nano-SiHA of divalent anions such as CO_3^{2-} or HPO_4^{2-} that can partially remain at 700ºC. After

the thermal treatment at 1150ºC, these anions would be fully substituted by PO_4^{3-} and SiO_4^{4-} thus resulting in more negative potentials at the materials surface.

Table 1. Textural properties and ζ potential of nano-SiHA and Si-HA

Sample	S_{BET} ($m^2 \cdot g^{-1}$)	Pore Volume ($cm^3 \cdot g^{-1}$)	Pore size (nm)	ζ potential (mV)
Nano-SiHA	25.9	0.17	26.8	-8.6
SiHA	1.23	0.003	6.4	-14.5

Figure 2 shows the proliferation values, cell viability and intracellular reactive oxygen species (ROS) content of Saos-2 osteoblasts after 24 h of culture on nano-SiHA and SiHA disks. Although this cell type proliferated on the surface of both biomaterials, the cell number and viability were significantly lower ($p < 0.05$) on nano-SiHA than on SiHA disks. Intracellular ROS levels were also significantly lower in contact with the nanocrystalline material ($p < 0.005$), thus revealing that the nanocrystallinity of SiHA did not induce oxidative stress in this cell type.

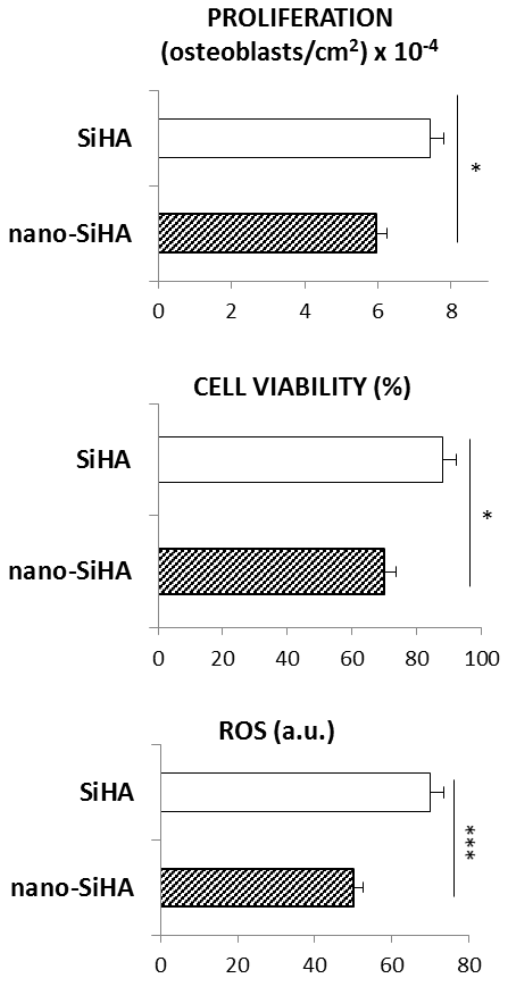

Figure 2. Effects of nano-SiHA and SiHA disks on proliferation, cell viability and intracellular reactive oxygen species (ROS) content of Saos-2 osteoblasts after 24 h of culture. * Comparison between each biomaterial. Statistical significance: *p < 0.05; *** p < 0.005.

In order to know if the decrease produced by nano-SiHA disks on the cell number was due to either cell cycle alterations or apoptosis, the cell cycle phases (G0/G1 = Quiescence/Gap1, S = Synthesis and G2/M = Gap2/Mitosis) of osteoblasts cultured on nano-SiHA and SiHA disks were evaluated by flow cytometry and SubG1 fraction (cells with fragmented DNA) was used as indicative of apoptosis. As it can be observed in Figure 3, the osteoblast SubG1 fraction was significantly higher (p > 0.01) on nano-SiHA disks than on SiHA disks. Nano-SiHA also induced significant decreases of both S (p > 0.05)

and G2/M ($p > 0.01$) phases in comparison with SiHA. These results evidence a slight but significant apoptosis increase and a cell cycle delay in response to the nanocrystalline material. Apoptosis is generally associated with the increase of intracellular reactive oxygen species (ROS) (32), however intracellular ROS levels were significantly lower ($p < 0.005$) in osteoblasts cultured on nano-SiHA than on SiHA disks (Figure 2). The apoptosis increase observed on nano-SiHA could be produced by insufficient and weak contacts between the osteoblasts and the nanocrystalline material surface which can trigger a kind of apoptosis defined as anoikis, induced by the loss of cell/matrix interactions (33-36). This process is important for development and tissue homeostasis, although it has been also related to several diseases (37). The possible loss of cell anchorage due to the nanocrystallinity of nano-SiHA has been also evaluated in the present study by confocal microscopy and scanning electron microscopy.

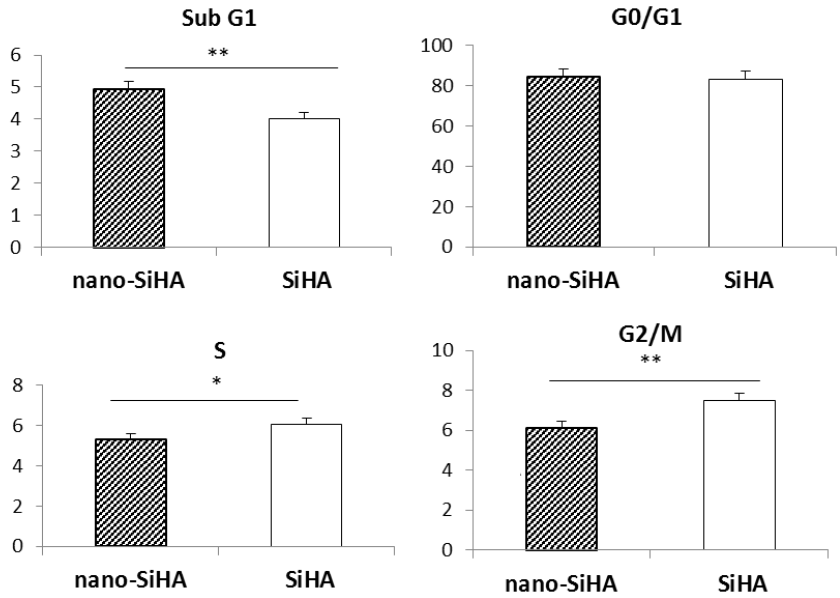

Figure 3. Effects of nano-SiHA and SiHA disks on cell cycle phases of Saos-2 osteoblasts after 24 h of culture. * Comparison between each biomaterial. Statistical significance: *$p < 0.05$; ** $p < 0.01$.

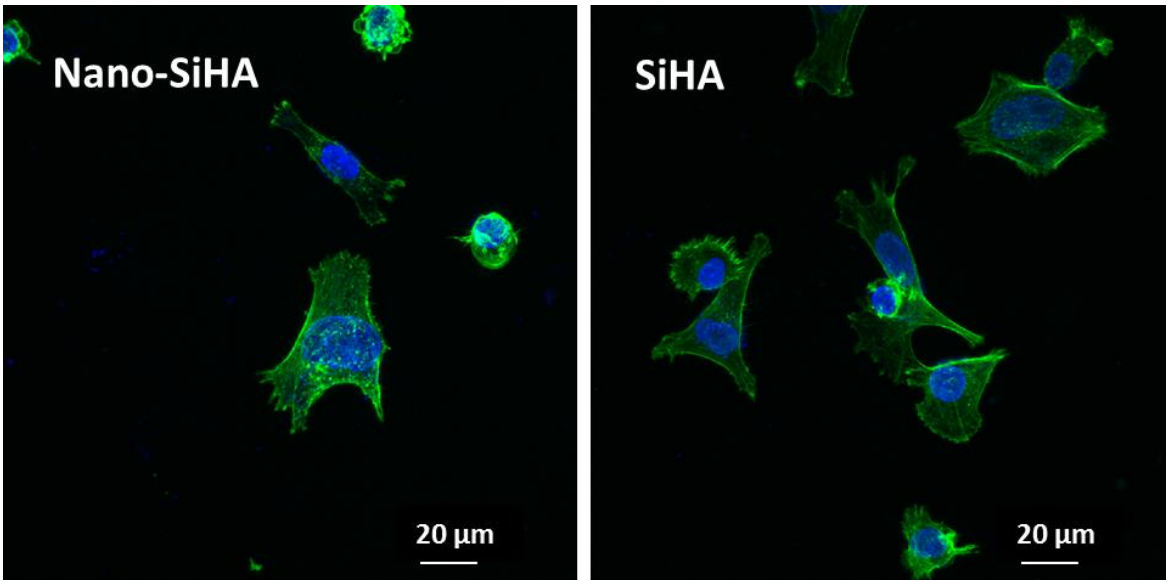

Figure 4. Morphology of Saos-2 osteoblasts on disks of nano-SiHA and SiHA observed by confocal microscopy after 24 h of culture. Actin was stained with FITC-phalloidin (green) and nuclei were stained with DAPI (blue).

Figure 4 shows the morphology of Saos-2 osteoblasts on nano-SiHA and SiHA disks observed by confocal microscopy after 24 h of culture. Actin filaments were stained with FITC-phalloidin (green) and nuclei were stained with DAPI (blue). Osteoblasts were well spread on the disk surface of both hydroxyapatites, with a distinctive actin network and presenting their correct morphology. However the cell number on nano-SiHA disks was lower than on SiHA disks. On the other hand, some cells showing spherical shape with diminished adhesion were observed on nano-SiHA disk surface revealing that the nanocrystalline material could produce anoikis. When Saos-2 osteoblasts cultured on nano-SiHA and SiHA disks were observed by scanning electron microscopy (SEM) after 24 h of culture, SEM images demonstrate the presence of cells attached on both materials, with the typical characteristics of osteoblast morphology (Figure 5). However, these SEM images demonstrate the presence of a higher number of cells attached on SiHA disks than on nano-SiHA, showing long cytoplasmic prolongations to adhere to the surface of SiHA disks. The decrease of the osteoblast number observed by SEM on nano-SiHA, in comparison with SiHA, is in agreement with the proliferation data (Figure 2) and with the confocal

microscopy images (Figure 4). These results indicate a good biocompatibility of both SiHA and nano-SiHA materials but a better interaction of osteoblasts with SiHA disks than with nanocrystalline SiHA disks.

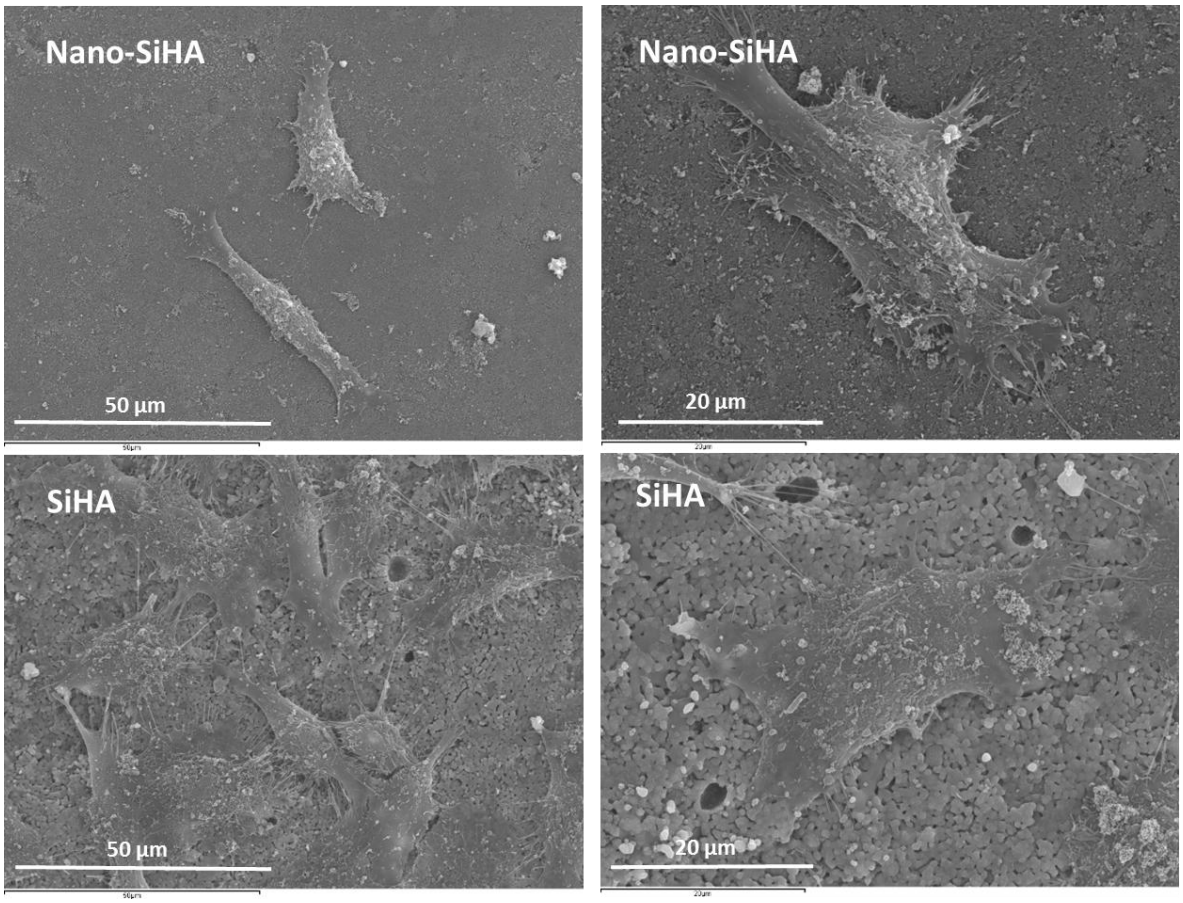

Figure 5. Morphology of Saos-2 osteoblasts on disks of nano-SiHA and SiHA observed by scanning electron microscopy after 24 h of culture.

Previous studies with nanocrystalline hydroxyapatites (nano-SiHA and nano-HA) showed that the substitution with Si delayed the osteoclast-like cell differentiation after 21 days of culture and decreased their resorptive activity without differences in cell viability (38). These results were probably due to the action of Si which can affect the late stages of differentiation and fusion of osteoclasts, causing *in vitro* a significant inhibition of osteoclast phenotypic gene expressions, osteoclast formation and resorptive activity (14). In the present study, in order to know the nanocrystallinity effects of nano-SiHA on the osteoclast differentiation and resorptive activity, murine RAW-264.7 macrophages were

cultured for 7 days on the surface of nanocrystalline (nano-SiHA) and crystalline SiHA disks and differentiated into osteoclast-like cells in the presence of soluble receptor activator of nuclear factor kappa-B ligand (RANKL) and macrophage/monocyte-colony forming factor (M-CSF). The shorter time of 7 days was chosen in order to know the effects of nanocrystallinity of nano-SiHA on the early osteoclast-like cell differentiation, avoiding the effects produced by Si on the late stages of differentiation (14,38).

Figure 6 shows the values of cell proliferation, viability and intracellular reactive oxygen species (ROS) of osteoclast-like cells after 7 days of culture on nano-SiHA and SiHA disks.

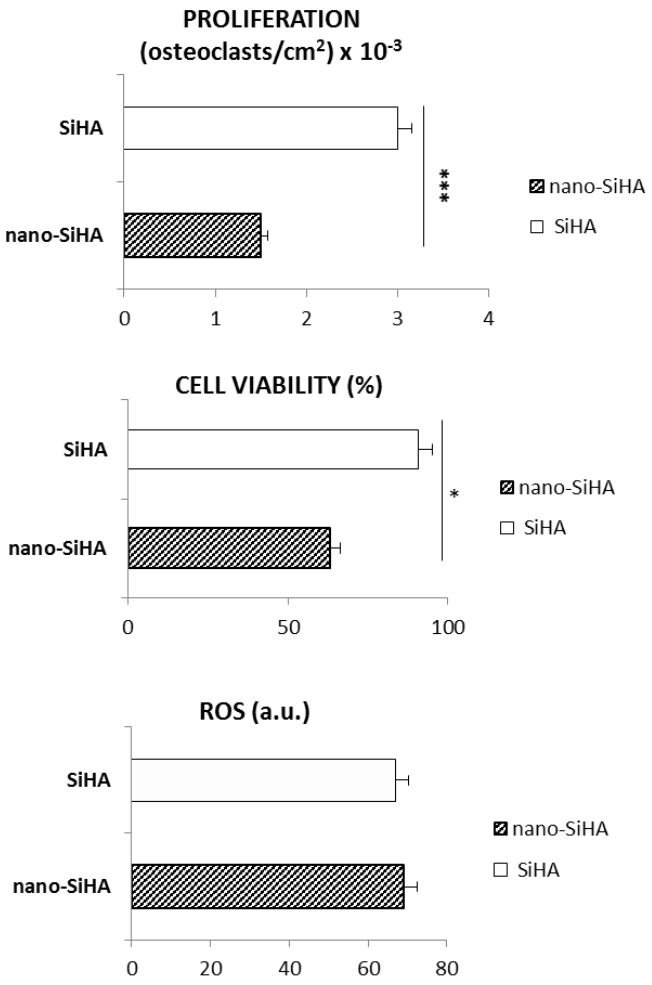

Figure 6. Effects of SiHA and nano-SiHA disks on proliferation, cell viability and intracellular reactive oxygen species (ROS) of osteoclast-like cells after 7 days of culture. * Comparison between each biomaterial. Statistical significance: *$p < 0.05$; *** $p < 0.005$.

The osteoclast-like cell number and viability were significantly lower ($p < 0.005$ and $p < 0.05$ respectively) on nano-SiHA than on SiHA disks. However, intracellular ROS levels were similar on both materials.

The morphology of osteoclast-like cells on disks of nano-SiHA and SiHA was observed by confocal microscopy and SEM after 7 days of culture (Figures 7 and 8 respectively).

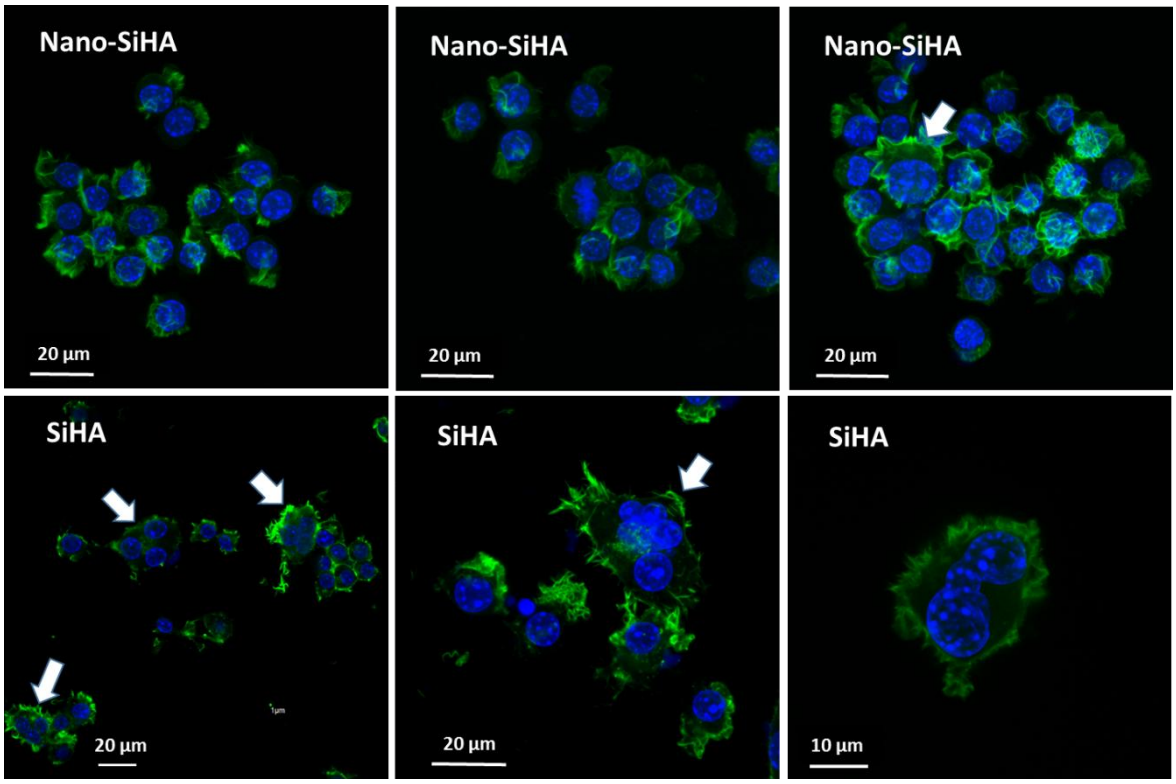

Figure 7. Morphology of osteoclast-like cells on disks of nano-SiHA and SiHA observed by confocal microscopy after 7 days of culture. Actin was stained with FITC-phalloidin (green) and nuclei were stained with DAPI (blue).

Multinucleated cells were observed on SiHA disks (Figure 7, arrows, lower panel) revealing osteoclast-like cell differentiation from RAW macrophages on the surface of this material after 7 days in the presence of RANKL and MSCF. However, multinucleated cells were not obtained on nano-SiHA disks after this treatment (Figure 7, upper panel), thus indicating that the nanocrystalline SiHA induced a delay of the osteoclast differentiation

process in comparison with the crystalline material. The formation of podosomes and the presence of actin rings, which define the sealing zone and are critical for the resorptive activity of this cell type, were also observed on SiHA disks but not on nano-SiHA disks.

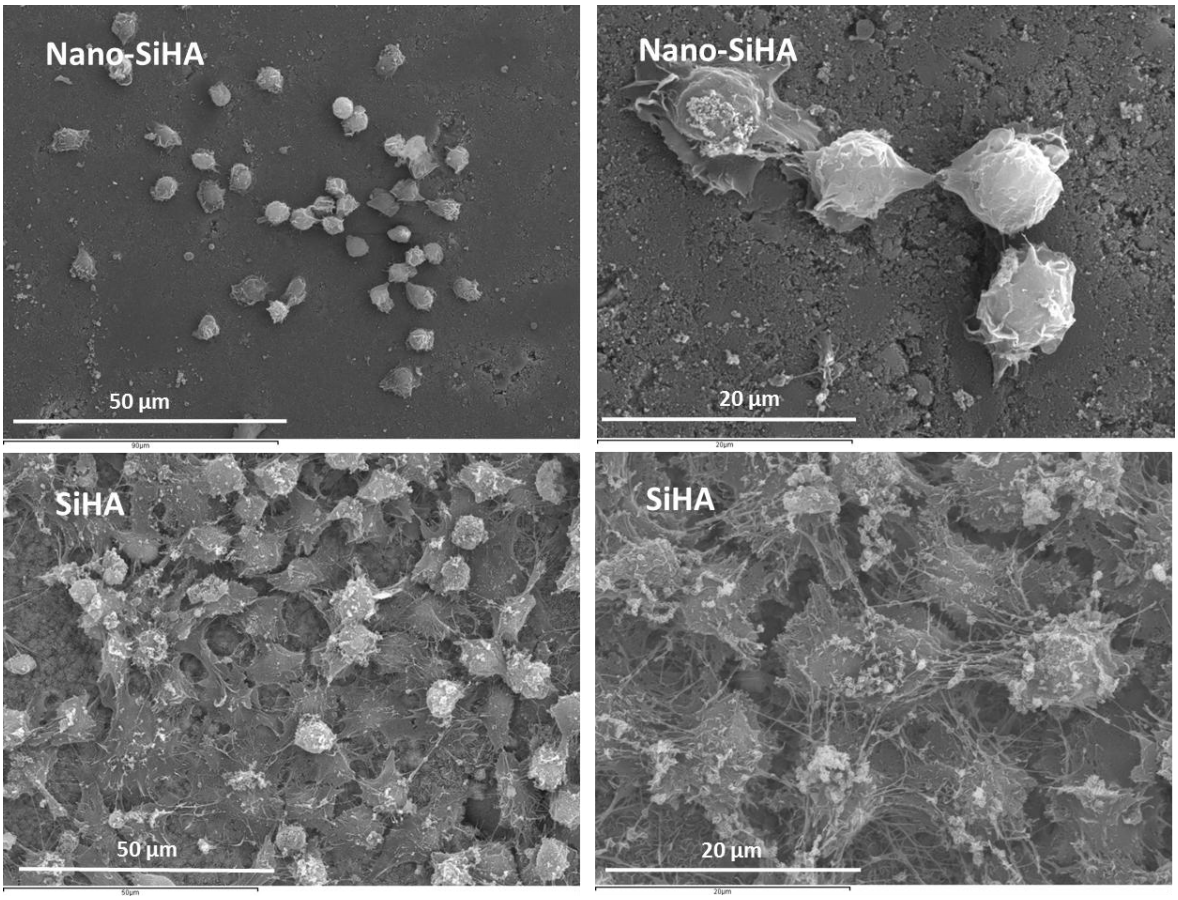

Figure 8. Morphology of osteoclast-like cells on disks of nano-SiHA and SiHA observed by scanning electron mycroscopy after 7 days of culture.

SEM studies showed the presence of a higher number of cells attached on SiHA disks than on nano-SiHA disks (Figure 8). The cells attached on SiHA disks present bigger size than on nano-SiHA disks and the typical characteristics of osteoclast-like cells with many longer podosomes. Cells on nano-SiHA show spherical shape with diminished adhesion which indicates the induction of anoikis by this material. Figure 9 shows the resorption cavities left by osteoclast-like cells cultured on nano-SiHA and SiHA disks after 7 days of

culture evaluated by SEM. The morphology and the number of these cavities evidenced that the resorptive activity were also higher on SiHA disks than on nano-SiHA disks.

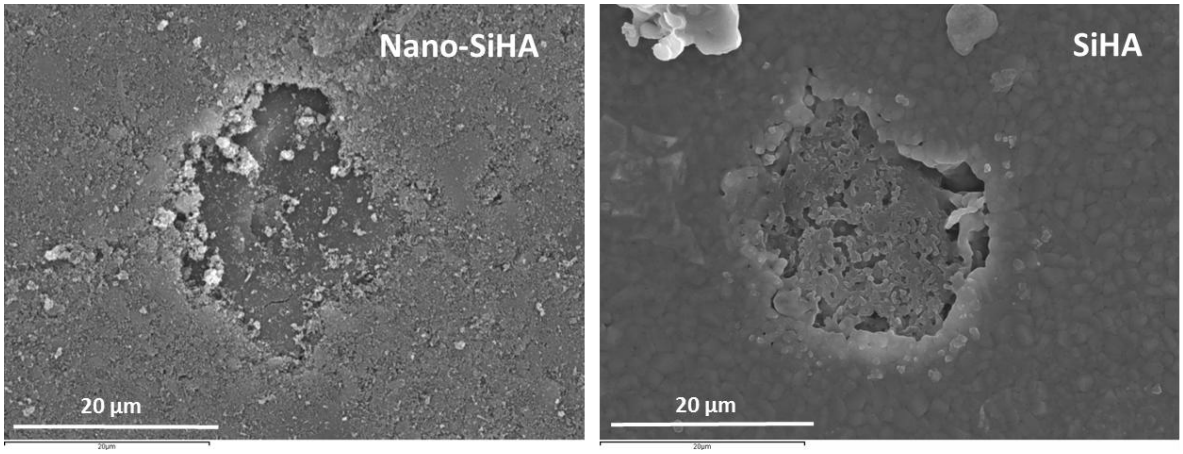

Figure 9. Morphology evaluation by scanning electron microscopy of the resorption cavities left by osteoclast-like cells cultured on nano-SiHA and SiHA disks after 7 days of culture.

All these results demonstrate that the different topography of nanocrystalline SiHA, in comparison with crystalline SiHA, induces anchorage loss of bone cells on its surface, delaying cell adhesion, proliferation, differentiation and activity. Concerning adsorption of serum proteins and fibrinogen, which could be related to the implant success and hemocompatibility, previous studies evidenced that the amount of both serum albumin and fibrinogen adsorbed on crystalline SiHA was significantly lower than on nanocrystalline SiHA (39).

4. Conclusions

Previous studies with nanocrystalline hydroxyapatites (nano-SiHA and nano-HA) showed that the substitution with Si delayed the osteoclast-like cell differentiation after 21 days of culture, decreasing their resorptive activity without affecting cell viability (38), probably due to the Si action on the late stages of differentiation and fusion of osteoclasts (14). In the present work, to know the nanocrystallinity effects of

nano-SiHA on both osteoblasts and osteoclasts, an *in vitro* comparative study between nano-SiHA and crystalline SiHA was carried out after a shorter time (7 days), evidencing that nanocrystallinity of silicon substituted hydroxyapatite affects the bone cell/biomaterial interface inducing bone cell apoptosis by loss of cell anchorage (anoikis), delaying early osteoclast-like cell differentiation and decreasing the resorptive activity of this cell type.

Since osteoclasts, as principal bone-resorbing cells, are involved in the pathogenesis of osteoporosis, these findings are of great interest in relation with the potential use of nanocrystalline silicon substituted hydroxyapatite for preventing bone resorption in treatment of osteoporotic bone. Mineralization studies with an osteopenic sheep model are currently being carried out for *in vivo* evaluation of these hydroxyapatites (project from Ministerio de Economía y Competitividad MAT2013-43299-R) and the obtained results will be included in a future manuscript.

Acknowledgments

This study was supported by research grants from the Ministerio de Ciencia e Innovación (project MAT2012-35556), Ministerio de Economía y Competitividad (project MAT2013-43299-R) and Agening Network of Excellence (CSO2010-11384-E). M.C. Matesanz is greatly indebted to MEC for predoctoral fellowship. The authors wish to thank also to the staff of the ICTS Centro Nacional de Microscopia Electrónica (Spain)) for the assistance in the scanning electron microscopy and to the staff of the Centro de Citometría y Microscopia de Fluorescencia of the Universidad Complutense de Madrid (Spain) for the assistance in the scanning electron microscopy and flow cytometry studies.

References

1. Parfitt AM. Targeted and nontargeted bone remodeling: relationship to basic multicellular unit origination and progression. Bone 2002;30:5-7.

2. Harada S, Rodan GA. Control of osteoblast function and regulation of bone mass. Nature 2003;423:349-55.

3. Mackie EJ. Osteoblasts: novel roles in orchestration of skeletal architecture. Int J Biochem Cell Biol 2003;35:1301-5.

4. Boyle WJ, Simonet WS, Lacey DL. Osteoclast differentiation and activation. Nature 2003;423:337-42.

5. Qin A, Cheng TS, Pavlos NJ, Lin Z, Dai KR, Zheng MH. V-ATPases in osteoclasts: structure, function and potential inhibitors of bone resorption. Int J Biochem Cell Biol 2012;44:1422-35.

6. Väänänen HK, Liu YK, Lehenkari P, Uemara T. How do osteoclasts resorb bone?. Mater Sci Eng C 1998;6:205-9.

7. Manolagas SC. Cellular and molecular mechanisms of osteoporosis. Aging 1988;10:182-90.

8. Luhmann T, Germershaus O, Groll J, Meinel L. Bone targeting for the treatment of osteoporosis. J Control Release 2012;161:198-213.

9. Carlisle EM. Silicon as a trace nutrient. Sci Total Environ 1998;73:95-106.

10. Schwarz K. A bound form of silicon in glycosaminoglycans and polyuronides. Proc Natl Acad Sci 1973;70:1608-12.

11. Carlisle EM. *In vivo* requirement for silicon in articular cartilage and connective tissue formation in the chick. J Nutr 1976;106:478-84.

12. Landis WJ, Lee DD, Brenna JT, Chandra S, Morrison GH. Detection and localization of silicon and associated elements in vertebrate bone tissue by imaging ion microscopy. Calcif Tissue Int 1986;38:52-9.

13. Reffitt DM, Ogston DN, Jugdaohsingh R, Cheung HF, Evans BA, Thompson RF, Powell JJ, Hampson GN. Orthosilicic acid stimulates collagen type 1 synthesis and osteoblastic differentiation in human osteoblast-like cells *in vitro*. Bone 2003;32:127-35.

14. Mladenović Z, Johansson A, Willman B, Shahabi K, Björn E, Ransjö M. Soluble silica inhibits osteoclast formation and bone resorption *in vitro*. Acta Biomater 2014;10:406-18.

15. Li H, Chang J. Bioactive silicate materials stimulate angiogenesis in fibroblast and endothelial cell co-culture system through paracrine effect. Acta Biomater 2013;9:6981-91.

16. Bouletreau PJ, Warren SM, Spector JA, Peled ZM, Gerrets RP, Greenwald JA, Longaker MT. Hypoxia and VEGF up-regulate BMP-2 mRNA and protein expression in microvascular endothelial cells: implications for fracture healing. Plast Reconstr Surg 2002;109:2384-97.

17. Shepherd JH, Shepherd DV, Best SM. Substituted hydroxyapatites for bone repair. J Mater Sci Mater Med 2012;23:2335-47.

18. Patel N, Best SM, Bonfield W, Gibson IR, Hing KA, Damien E, Revell PA. A comparative study on the *in vivo* behavior of hydroxyapatite and silicon substituted hydroxyapatite granules. J Mater Sci Mater Med 2002;13:1199-206.

19. Pietak AM, Reid JW, Stott MJ, Sayer M. Silicon substitution in the calcium phosphate bioceramics. Biomaterials 2007;28:4023-32.

20. Bohner M. Silicon-substituted calcium phosphates - a critical view. Biomaterials 2009;30:6403-6.

21. Balas F, Pérez-Pariente J, Vallet-Regí M. *In vitro* bioactivity of silicon-substituted hydroxyapatites. J Biomed Mater Res A 2003;66:364-75.

22. Porter AE, Best SM, Bonfield W. Ultrastructural comparison of hydroxyapatite and silicon-substituted hydroxyapatite for biomedical applications. J Biomed Mater Res A 2004;68:133-41.

23. Dvorak MM, Siddiqua A, Ward DT, Carter DH, Dallas SL, Nemeth EF, Riccardi D. Physiological changes in extracellular calcium concentration directly control osteoblast function in the absence of calciotropic hormones. Proc Natl Acad Sci 2004;101:5140-5.

24. Porter AE, Patel N, Skepper JN, Best SM, Bonfield W. Comparison of *in vivo* dissolution processes in hydroxyapatite and silicon-substituted hydroxyapatite bioceramics. Biomaterials 2003;24:4609-20.

25. Matesanz MC, Feito MJ, Ramírez-Santillán C, Lozano RM, Sánchez-Salcedo S, Arcos D, Vallet-Regí M, Portolés MT. Signaling pathways of immobilized FGF-2 on silicon-substituted hydroxyapatite. Macromol Biosci 2012;12:446-53.

26. Balamurugan A, Rebelo AHS, Lemos AF, Rocha JHG, Ventura JMG, Ferreira JMF. Suitability evaluation of sol-gel derived Si-substituted hydroxyapatite for dental and maxillofacial applications through in vitro osteoblasts response. Dent Mater 2008;24:1374-80.

27. Arcos D, Rodríguez-Carvajal J, Vallet-Regí M. Silicon incorporation in hydroxylapatite obtained by controlled crystallization. Chem Mater 2004;16:2300-8.

28. Dorozhkin SV. Nanodimensional and nanocrystalline apatites and other calcium orthophosphates in Biomedical Engineering, Biology and Medicine. Materials 2009;2:1975-2045.

29. Thian ES, Ahmad Z, Huang J, Edirisinghe MJ, Jayasinghe SN, Ireland DC, Brooks RA, Rushton N, Bonfield W, Best SM. The role of surface wettability and surface charge of electrosprayed nanoapatites on the behaviour of osteoblasts. Acta Biomater 2010;6:750-5.

30. Samaved S, Whittington AR, Goldstein AS. Calcium phosphate ceramics in bone tissue engineering: a review of properties and their influence on cell behavior. Acta Biomater 2013;9:8037-45.

31. Bohner M, Lemaitre J. Can bioactivity be tested *in vitro* with SBF solution?. Biomaterials 2009;30:2175-9.

32. Quillet-Mary A, Jaffrezou JP, Mansat V, Bordier C, Naval J, Laurent G. Implication of mitochondrial hydrogen peroxide generation in ceramide-induced apoptosis. J Biol Chem 1997;272:21388-95.

33. Frisch SM, Ruoslaht E. Integrins and anoikis. Curr Opin Cell Biol 1997;9:701-6.

34. Frisch SM, Screaton RA. Anoikis mechanisms. Curr Opin Cell Biol 2001;13:555-62.

35. Grossmann J, Walther K, Artinger M, Kiessling S, Scholmerich J. Apoptotic signaling during initiation of detachment-induced apoptosis ("anoikis") of primary human intestinal epithelial cells. Cell Growth Differ 2001;12:147-55.

36. Alcaide M, Serrano MC, Román J, Cabañas MV, Peña J, Sánchez-Zapardiel E, Vallet-Regí M, Portolés MT. Suppression of anoikis by collagen coating of interconnected macroporous nanometric carbonated hydroxyapatite/agarose scaffolds. J Biomed Mater Res A 2010;95:793-800.

37. Chiarugi P, Giannoni E. Anoikis: a necessary death program for anchorage-dependent cells. Biochem Pharmacol 2008;76:1352-64.

38. Matesanz MC, Linares J, Lilue I, Sánchez-Salcedo S, Feito MJ, Arcos D, Vallet-Regí M, Portolés MT. Nanocrystalline silicon substituted hydroxyapatite effects on osteoclast differentiation and resorptive activity. J Mater Chem B 2014;2:2910-9.

39. Matesanz MC, Linares J, Oñaderra M, Feito MJ, Martínez-Vázquez FJ, Sánchez-Salcedo S, Arcos D, Portolés MT, Vallet-Regí M. Response of osteoblasts and preosteoblasts to calcium deficient and Si substituted hydroxyapatites treated at different temperatures. Colloids Surf, B 2015;133:304-13.